We would like to thank the reviewers for their insightful commentary and catching the inconsistencies that existed in the first version. As a result, we have revised the manuscript substantially and believe it has significantly improved from its original submission. Please see the tracked changes revision attached to this review. One change that we made on our own volition was to develop a separate sub-category of the southeasterly cases that were either completely or predominantly southeasterly, and were either SDE days (i.e., 24 Feb and 10 Mar) or days with the most boundary layer influence based on the radon data (i.e., 27 Feb and 28 Feb). These days are indicated in green in the table, and figures and discussion has been revised to reflect this change.

Summary:

The two related goals of the paper are: in-cloud measurements of INPs and the identification of INP type or composition. The paper makes a good contribution to INP studies by providing a data set involving INP measurements in air (with size sorting), rime, and snow at the same time. They show evidence for the dependence of INP abundance depending of air mass trajectory. Some inferences are drawn regarding local versus distant sources of INPs. The authors' conclusions are relatively simple and reasonably well supported by the data, but the analyses are limited without chemical and other supporting measurements. All that notwithstanding, an important revision is needed to take into account the points made in the Section 3 below.

Major remarks:

1) Stratification by storm type in Sections 3.1 and 3.2 focus only on air trajectory. It is surprising that precipitation during 10 preceding days, cloud height, depth etc. are not considered. In some fashion those parameters are probably related to the airmass trajectories, but omission of attention to those factors makes the arguments presented sound incomplete and superficial. This sort of narrow focus in the treatment of the data is unsettling in various parts of the paper. Results in Section 3.2 and Fig. 6 are presented without separation of in-cloud and out-of-cloud samples. This sort of problem is not unique to this data set. It has also been there with the numerous papers reporting INP, and other, measurements at JFJ observatory.

The intention of the classification was to simply determine directionality of the storms—and thus, possible INP sources—affecting Jungfraujoch during the study as delineated by section 3.1. The two dominant flow patterns are well documented at Jungfraujoch (i.e., Stopelli et al. (2015) and the newly-added reference of Collaud Coen et al. (2011)). In the current work, we use air mass trajectories, but also corroborate with local wind speed and direction, and evaluate INPs in the context of air temperature during storm days in section 3.2.

We do not classify by "storm type" since adequate parameters such as precipitation quantities and cloud properties were not measured and are not routine baseline measurements at Jungfraujoch. For clarity, we now provide a definition of "storms" in the beginning of section 3.1: "These days were also deemed days with "storm" conditions since clouds and snow were both present at JFJ." We also now define that we evaluate INPs in the context of storm directionality where appropriate throughout the revision (e.g., in section 3.2). However, we have included some non-storm days in the revision and initially define those in section 3.1, so we have reduced the use of "storm" cases unless only referring to the northwest or southeast samples.

We already presented cloud percentage data in Figures 1 and 8 (now presented in the new Figure 1 only) using the methodology of Herrmann et al. (2015), which show that all case study samples were collected under at least some percentage of in-cloud conditions. This agrees with the fact that cloud rime was collected during our case study days, indicating the presence of clouds. Presenting the cloud data a third time in Figure 6 would be redundant.

Collaud Coen, M., Weingartner, E., Furger, M., Nyeki, S., Prevot, A. S. H., Steinbacher, M., and Baltensperger, U.: Aerosol climatology and planetary boundary influence at the Jungfraujoch analyzed by synoptic weather types, Atmos Chem Phys, 11, 5931-5944, 10.5194/acp-11-5931-2011, 2011.

2) The paper expands on other INP data from JFJ by determining INP abundance as a function of temperature, i.e. INP spectra. This is a useful step and avoids the somewhat simplistic comparisons that, unfortunately, arise from discussing and comparing INP concentrations without distinguishing between data obtained at -10°C or at -30°C. INP composition, their sources and their transport can be expected to be significantly different for widely different temperature regimes. The greater focus on this aspect of INP studies is a good contribution. Expanding further on the point, use of differential INP spectra for gaining more information about INPs is a commendable goal as it goes even further in focusing on INP characteristics than the more frequently employed cumulative spectra. However, the manner this is done in this paper deserves closer examination and revision, as argued under the heading "Differential spectra" below.

We have revised the differential spectral calculations, figures, and discussion significantly to follow the methodology of Vali (2018). Please see detailed responses in the "Differential spectra" section below.

3) As a general comment about interpretations of INP spectra, I'd express some caution. The paragraph in lines 267-285 about warm and cold-mode INPs is somewhat superficial. The temperature ranges and magnitudes of INP concentrations need to be considered quantitatively before deductions are made about possible sources of the INPs. Just looking at freezing temperatures (like onset and percentiles frozen) can be misleading since they depend on sample concentration (e.g. filter exposure time, dilution), number of drops tested and drop volume.

We now chiefly focus on the differential spectra but still do mention the cold and warm modes in the original df/dT spectra, which are now correctly labeled. We have found df/dT useful in qualitative evaluation of possible different INP populations (i.e., what are likely modes for mineral + biological versus biological) within one sample, as demonstrated additionally in previous work by Augustin et al. (2013). Almost all of the samples (except for the 24-Feb and 28-Feb aerosol samples) contain spectra that have a cold mode when assessing df/dT, but we would like to show their temperatures to demonstrate the dT between each of the two modes when a warm mode is present. The warm mode in the differential spectra afford a more quantifiable approach of the "bump" in the warm regime of the cumulative spectra as observed in previous studies (e.g., DeMott et al., 2016; DeMott et al., 2018; Hill et al., 2016; Kanji et al., 2017; McCluskey et al., 2017; Petters and Wright, 2015; Suski et al., 2018; Vali, 1971; Vali and Stansbury, 1966).

Hence, we decided to show both spectra types in addition to cumulative and have clarified throughout the text which we refer to. We also have added explanation and discussion on all three types of spectra and why they are useful in section 3.2. The new Figure 5 contains all three spectra types, but Figure 6 shows mode temperatures for df/dT since the differential spectra have the same values for the warm mode (as we now note in the caption and discussion) and no mode in the cold regime due to exponential increase at those temperatures. We use this combination of spectral information to glean possible sources.

Augustin, S., Wex, H., Niedermeier, D., Pummer, B., Grothe, H., Hartmann, S., Tomsche, L., Clauss, T., Voigtländer, J., Ignatius, K., and Stratmann, F.: Immersion freezing of birch pollen washing water, Atmos. Chem. Phys., 13, 10989-11003, 10.5194/acp-13-10989-2013, 2013.

4) Related to the point raised in 1), one wonders what is underlying vision for comparing or correlating INP concentrations in air (via the filters) and in snow and in rime. These are three very different pathways for

the INPs. Sources for each component can be different in space and time. With a broad separation such as NW versus SE airmasses perhaps these differences become unimportant but not necessarily so. It would be useful to read about the authors' perception on this issue. The paper glosses over such concerns thereby creating a degree of unease about the meaning of the results.

The difference in temporal coverage between snow, rime, and aerosol sampling was due to practical constraints. It forces us to integrate in our interpretation over an air mass including clouds and cloud-free sections. As long as wind direction and planetary boundary layer influence are similar within an air mass, we think this approach can still lead to insights, although a perfect synchrony in sampling all components would of course have been preferable. We now address this issue at the end of section 2.1 (Aerosol, cloud rime and snow collection at Jungfraujoch).

Differential spectra:

5) What in this paper is called (Fig. 7, lines 26, 145, and other places) "normalized differential INP concentration" does not correspond to previously used definitions of that term. Earlier definitions are found in the references cited in the paper. Further references are Vali et al. (2015) (Atmos. Chem. Phys. 15, 10263-10270) and the recent Vali (2018) (Atmos. Meas. Tech. 15 Discuss., https://doi.org/10.5194/amt-2018-309). To summarize, briefly, differential spectra, or differential INP concentrations, reflect the concentration of INPs or active sites per unit temperature interval. It also describes the probability of freezing for drops of given volume at given temperatures. As its name indicates, the differential spectrum corresponds to the differential of the cumulative spectra. The cumulative spectrum is denoted by [INPs(T)] on line 147 of the paper. Other frequent designation of this cumulative spectrum is K(T), with k(T) used for the differential spectrum. Both quantities are closely related to site density. Because the values are specific to each temperature, independently of what other INPs may be present in the sample, the differential spectra provide more acute diagnoses of INP characteristics then the more frequently employed cumulative spectra or the fraction frozen.

We have revised the terminology to be consistent with Vali (2015, 2018). Specifically, we redefined cumulative INP concentrations or what we called [INPs(T)] as K(T) and differential INP concentrations as k(T). We relabeled axes in the figures and updated the text to be consistent with these definitions, and added more details on the calculations used in section 2.2 for clarity.

6) Line 152 states that differential values were obtained from the cumulative concentration. In fact, the results shown in Fig. 7 (right hand panels) and then used in Section 3.3 appear to represent some different quantity because differential spectra k(T) usually exhibit a steady rise with decreasing temperatures at low temperatures. The large drop in the spectra at low temperatures seen in the right-hand panels of Fig. 7 suggest that what is shown in the graphs represent the differentials of the frequency of freezing events, f(T), not of the cumulative INP concentration. Since fewer and fewer drops are left as the sample drops freeze and f(T) approaches unity at the lowest temperatures in an experiment, the increase in f(T) per temperature interval, δf(T)/δT, can be expected to drop off, just as it seen in these figures.

We realize we had previously only shown the differential of f(T) (i.e., δf(T)/δT or df/dT as we call it to be consistent with the notation presented by Augustin et al. (2013))—thank you for catching this inconsistency. We redid all calculations and now provide the k(T) equation from Vali (2018) that we applied to our data (see section 2.2). We now show K(T), df/dT, and k(T) in the new Figure 5.

Bimodality was evident in the df/dT spectra, however, given the large increase in k(T) in the cold temperature (i.e., < −15 °C) regime, well-defined "cold modes" are not present. We now clarify that when we refer to cold modes, that is for df/dT only and warm modes are for both df/dT and k(T). We have highlighted these regions in each of the spectra types in Figure 5.

7) The differential δf(T)/δT is a valid representation of the measurements but it lacks clear physical meaning. That differential is nearly the same as the 'freezing rate, R(T)' defined in Section 4.6 of Vali et al. (2015), but without the first ratio in that definition. For f(T) << 1, i.e. at the higher (warm) end of the range δf(T)/δT the first term in R(T) is close to unity and δf(T)/δT ~ R(T) so that minor peaks are resolved in δf(T)/δT without the distorting effect of reduced sample size. However, at smaller values of f(T) that distortion becomes dominant, so that little significance can be attached to peaks such as those shown in Fig. 7 of the paper. That this is indeed the case can be demonstrated by changing the drop volumes. Such a change would shift the positions of the cold-mode peak. In contrast, k(T) for different drop sizes overlap and form a continuous curve (e.g. Fig. 4 in Vali (1971)(J. Atmos. Sci., 28,402). Another illustration can be thought of with dilutions of the sample with INP-free water. The drop-off beyond the cold-mode peak of the original sample will not be reproduced with the diluted sample since large numbers of drops will be still available for substantial rates of freezing at that temperature. In this case too, k(T) for successive dilutions overlap and form a continuous curve. The ratio δf(T)/δT has not been used in the past to describe experimental results, so the authors should define it clearly and explain why they chose that presentation. Renaming that quantity would be helpful in avoiding future misunderstandings. Alternatively, they could consider changing the analysis to using k(T) or R(T) to represent their data. The point is that δf(T)/δT is an experiment-specific relative characterization of the results, while other, more objective quantities could be used. An additional effect of the choice of analysis in terms of δf(T)/δT is that freezing of some of the drops at warmer temperatures decreases the number and, potentially, the gradient of the frequency at lower temperatures. Is that the reason why the so-called cold-mode for the SE samples seems to occur at warmer temperatures in Fig. 7 than for the NW samples?

We have found df/dT useful in qualitative evaluation of possible different INP populations (i.e., what are likely modes for mineral + biological versus biological) within one sample, as demonstrated additionally in previous work by Augustin et al. (2013). We realize this may be experiment-specific and make note of this in section 3.2 – that the use of df/dT is to intercompare samples in this study. We are now careful with discussion on these spectra and are transparent by explaining their qualitative nature of showing either one or two of the INP populations.

Specific remarks:

lines 33-34: Precipitation production is not limited, as implied, to clouds that contain both liquid and ice, Unfortunate phrasing. But the mention of mixed-phase clouds (MPC) in the subsequent several lines keep mixing the focus on the importance of INPs in general and the importance of MPCs for precipitation production.

For clarity, we have changed this sentence to, "Aerosol-induced ice microphysical modifications influence cloud lifetime and albedo (Albrecht, 1989; Twomey, 1977; Storelvmo et al., 2011), as well as the production of precipitation (DeMott et al., 2010)."

line 37: There is jump here from the discussion of the INPs as important problems for weather and climate models to the practical problem of measuring INPs. Also, from none of the foregoing follows the argument of line 41 that in-cloud measurements are indispensable for progress.

We moved around a couple of sentences in this paragraph to start with only broader aerosol-cloud statements and then transition to INPs. We also changed "necessary" to "useful for assessing" to omit any idea that these are merely indispensable for progress.

line 43: Another jump in logic. What's said here had to be already taken for granted for the previous paragraph to make sense.

Because we reorganized this paragraph, we left the last sentence as it demonstrates that INP observations in-cloud are even more limited than observations in general (i.e., in both in-cloud and below-cloud or ground level measurements when measurements are not conducted at levels where clouds can form). Perhaps there is some confusion with "in cloudy" compared to "in-cloud". We have now clarified we are referring to directly in-cloud.

lines 43-76: These two paragraphs get into too much detail. The present study does not address many of the details described as possibly controversial or uncertain, so raising the issues is a diversion. Other review papers deal with what is known about the components of INPs. This paper is directed only to a broad classification of INP types by composition.

To provide context for the spectral characteristics and what they might mean, we need such detailed background on what types of INPs call where on the spectrum of freezing temperatures. However, we realize we cannot address the limitations that we call out from previous studies, so we remove mentioning of those uncertainties or controversial nature. We retain the limitations of the modeling examples, as they support the need for additional observations (not just ours, but in general, more are needed to improve the models).

lines 104-105: To what extent did wind removal of snow from the pans hinder determinations of snowfall rates?

Unfortunately, we can only speculate that winds did remove some of the snow but cannot quantitatively assess this to provide actual snow rates. We note wind removal is a possibility and thus cannot determine snowfall rates in the beginning of section 2.1.

line 131: Drop size variability introduces errors due to INP content being proportional to volume, as also pointed out in Creamean et al. 2018b. How significant this error is depends on the range of variation of drop volumes. The way this line is phrased is incorrect and subjective. The error introduced may be small or equal compared to other sources. The only concise way to test for this would be to do large numbers of repeated runs from the same sample. Recommend to change "indeterminable" to "undetermined" in line 130 and eliminate line 131.

Done.

line 136: Cooling-rate dependence is small but not non-existent as shown in the references cited. If the authors' tests showed no discernible dependency it must be because other variations hid the cooling-rate dependence.

Good point. We have changed "no discernible" to "very little discernible".

line 142: The reader deserves to know what this 'custom software' was that connects visual detection with a recording system. Also, one wonders why is cooling rate considered a factor for each drop, when the previous paragraph states that there is no 'discernible' effect.

It is simply software that records the time, probe temperature, and cooling rate every second. When we identify that a drop has frozen, we click a button so that the software records that exact time, probe temperature, and cooling rate of that drop in a separate file. We now provide this level of detail here.

line 144: How were triplicate samples combined for analyses? Averages of fraction frozen at each temperature? How much variability was there among the three runs per sample?

We have defined in our previous publications that the 3 tests typically do not vary drastically from each other, and any variability is considered when calculating the error bars. We first combine the frozen drop records from the three tests, then calculate fraction frozen, then INP concentrations. We have clarified this in section 2.2.

line 153: Assigning significance to the fact that the data shown in the references cited extended to only about -20°C may indicate a misunderstanding. The -20°C limit was due to no fundamental limitation of the validity of definition of differential spectra. It was due to the background from distilled water and from the supporting surface becoming important at colder temperatures.

Thank you for pointing this out. We have changed this sentence to, "Spectra from these previous studies only reached a minimum of –20 °C due to the limitations of background artifacts in the water used at that time."

lines 160-163: Can the method used distinguish between clouds enveloping the observatory and clouds just a few hundred meters above it? Were there no in-situ instruments or visibility measurements available for detection of clouds?

Unfortunately, there were no in situ cloud or visibility measurements. We added a statement delineating this missing element in the beginning of section 2.3. The effective sky temperature method we used from Hermann et al. (2015) demonstrates robustness in the winter at Jungfraujoch when compare to all-sky camera observations of cloud (i.e., both the method and all sky determine Jungfraujoch is in cloud 38% of the time in the winter), indicating the reliability of this method especially during this season. However, we cannot distinguish between clouds enveloping at the observatory and clouds a few hundred meters above. Given the scale of the storms hitting the site during INCAS (as evaluated from MODIS visible imagery; see representative examples from 15 Feb (top) and 24 Feb (bottom) below from https://worldview.earthdata.nasa.gov/), it is likely that the localized orographic formation is rare in comparison, rendering the issue irrelevant.
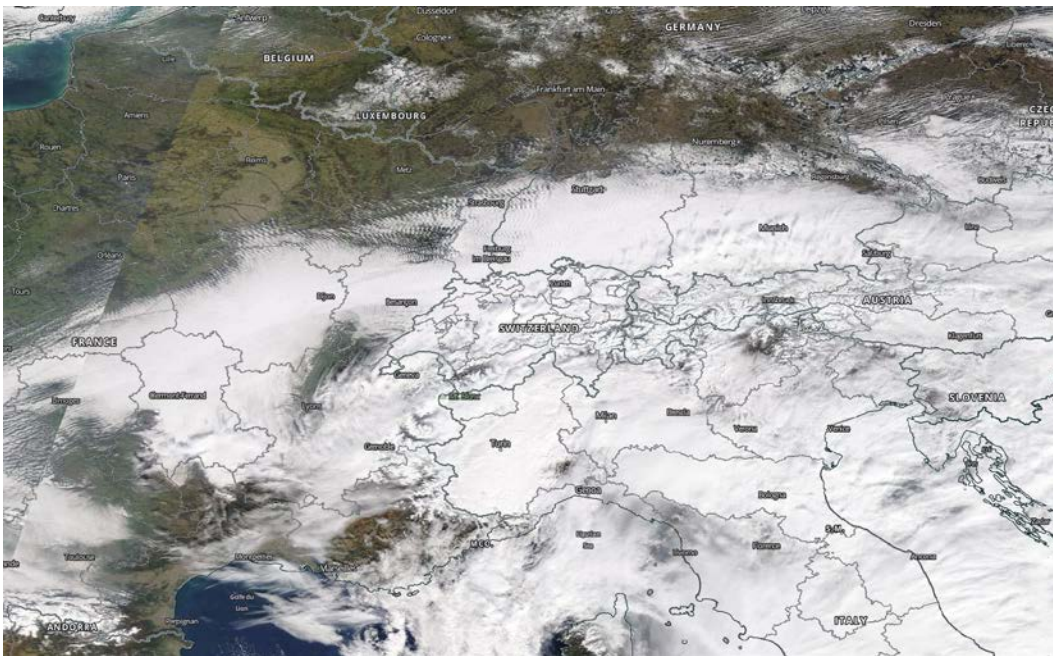
line 173: Please define SDE.

SDE was already defined in the introduction.

Fig. 6 panel a: Are the lines shown averages for the each condition? If the curves in panel a) are differential concentrations, as the presence of a peak suggests, then the units of the ordinate are incorrect.

These were averages of cumulative spectra. We originally did not include zero as INP values before the onset freezing temperatures, which is why it did not look correct or have a cumulative shape. We have fixed this and now label the plots to define when they are cumulative or otherwise.

Fig. 6 panel b-h: The numbers of points doesn't seem to be the same in each panel. Some points may be missing for samples that had no freezing event at -10°C, but shouldn't the other panels contain the same numbers of points. It is hard to tell if that is the case. Perhaps due to overlap of points. Please check and explain if some additional selection has been made.

This is due to overlap of some points, which we now state in the caption: "Some data points overlap and thus plots may appear to not have the same number of points per sample."

line 233->: It would be helpful if the authors stated what signals they consider significant in Fig. 6. The figure is complex and the data noisy. The jump into comparisons with the Stopelli data is hard to follow without first pointing out what deductions are extracted from Fig. 6.

We have significantly changed Figure 6 to make it less complex and noisy and now discuss it after showing the three different types of spectra. We segue from Figure 5 (spectra) to Figure 6 (statistics) more smoothly now so that the comparison with Stopelli et al. (2016) data make sense.

lines 239-240: The phrasing could be improved. You mean cumulative concentrations at -15°C as the criterion used for the assertion?

We did mean cumulative and now define this. Anytime we mention "INP concentrations", we now define it we are talking about cumulative or differential.

line 243: Onset definition is based on single drops? Wording in parenthesis on lines 244-245 should be corrected and made more specific.

Yes. We have no clarified this.

lines 265-266: This assertion about the role of hoar frost needs some explanation.

We have added to this sentence that hoar frost is a form of rime. Therefore, any addition of hoar frost to a collected snow sample will make it more similar to rime.

lines 267-285: This paragraph will need to be revisited after the authors examine the issue raised about the differential spectra, and also take into account the comment on line 153 above.

Done. This entire section was revised based on the addition of the correct differential spectra.

Section 3.3: Because of misgivings about the meaning of the cold-mode data, it is difficult to sort out what part of the conclusions is supported by the data. Focusing only on whether a minor peak was present or not and forgetting about the cold-mode W entries in Fig. 8 the analysis may not change much since the position of the C peaks is almost uniform for all the days and contains little additional information.

We have significantly revised this section to better explain what the results show by using a combination of cumulative, df/dT, and differential spectra.

line 348: Reference to 'differential INP spectra' need change in light of Section 3 of these comments.

We have fixed this to include the correct deductions based on the df/dT and correct differential spectra.

line 351: The meaning of statements about the relative magnitudes of INP concentrations is unclear unless the temperature to which they refer is specified, and it is clear what quantity is used for the comparison (f(T) or k(T) or K(T), or other).

We have defined the INP type, here and elsewhere in the manuscript for any mention of INP concentrations.

line 352: Reference to bi-modal spectra may also need to be re-thought depending on what changes are made regarding the use of δf(T)= δT) or its replacement. The line 354-359: The thoughts expressed here are basically sound but are somewhat overstated regarding how much information can be gained from cumulative versus differential spectra. The latter are more specific and make it easier to see differences among samples, but the information content is not different.

Based on the new calculations, our conclusions have been revised to properly fit what the data show.

Using **freezing** spectra characteristics to identify ice nucleating particle populations during **the** winter ~~storms~~ in the Alps

Jessie M. Creamean[1,2*], Claudia Mignani[3], Nicolas Bukowiecki[4**], Franz Conen[3]

[1]Cooperative Institute for Research in Environmental Sciences, University of Colorado, Boulder, CO, USA
[2]Physical Sciences Division, National Oceanic and Atmospheric Administration, Boulder, CO, USA
[3]Department of Environmental Sciences, University of Basel, Switzerland
[4]Laboratory of Atmospheric Chemistry, Paul Scherrer Institute, Villigen, Switzerland
[*]Now at: Department of Atmospheric Science, Colorado State University, Fort Collins, CO, USA
[**]Now at: 3

Email: jessie.creamean@colostate.edu

Abstract. One of the least understood cloud processes is modulation of their microphysics by aerosols, specifically of cloud ice by ice nucleating particles (INPs). To investigate INP impacts on cloud ice and subsequent precipitation formation, measurements in cloud environments are necessary but difficult given the logistical challenges associated with airborne measurements and separating interstitial aerosol from cloud residues. Additionally, determining the sources of INPs is important given the dependency of glaciation temperatures on the mineral or biological components and diversity of such INP populations. Here, we present results from a comparison of INP spectral characteristics in air, cloud rime, and fresh fallen snow ~~for storm days~~ at the High -Altitude Research Station, Jungfraujoch. The goal of the study was two-fold: (1) to assess variability in wintertime INP populations found in-cloud based on ~~air mass~~wind and air mass direction during snowfall and (2) to evaluate possible INP sources ~~s~~ between different sample types using a combination of cumulative INP ($K(T)$), normalized differential fraction frozen (df/dT), and normalized differential ~~differential~~ INP ~~spectra~~($k(T)$) spectra. INP freezing temperatures and concentrations were consistently higher on average from the southeast as compared to the northwest for rime, snow and especially aerosol samples which is likely a result of air mass influence from predominantly boundary layer terrestrial and marine sources in Southern Europe, the Mediterranean, and North Africa. For all three sample types combined, average onset freezing temperatures were −8.0~~7.7~~ and −11.3~~2~~ °C for southeasterly and northwesterly days, respectively, while $K(T)$ ~~INP concentrations~~ were 3 to 20 times higher when winds arrived from the southeast. Southeasterly aerosol samples typically had ~~bimodal freezing spectra~~a clear mode in the warm temperature regime (i.e., ≥ −15 °C) in the df/dT and $k(T)$ spectra—indicating a putative influence from biological sources—while ~~bimodality~~ the presence of a warm mode in ~~of~~ the rime and snow varied ~~depending on meteorological context~~. Evaluating df/dT~~normalized concert with~~ ~~differential INP spectra~~$k(T)$ spectra exhibited variable modality and shape—depending on the types of INPs present—and may serve as a ~~viable~~useful method for comparing different sampl~~ing~~e substances and assessing the possible relative contributions of mixed mineral and biological versus only biological ~~contributions to INP~~INP sample populations.

1 Introduction

Aerosols are key players in the atmospheric radiation budget, cloud microphysics, and precipitation development. ~~However, one of the most significant challenges with regard to aerosols is quantifying their impacts on cloud ice formation through serving as ice nucleating particles (INPs) (Boucher et al., 2013).~~ Aerosol-induced ice microphysical modifications influence cloud lifetime and albedo (Albrecht, 1989; Twomey, 1977; Storelvmo et al., 2011), as well as the production of precipitation (DeMott et al., 2010)~~in clouds containing both liquid and ice~~. Mixed-phase clouds (MPCs) are ubiquitous in the troposphere over the entire annual cycle yet are difficult to quantify globally in part due to an inadequate understanding of aerosol-cloud interactions in mixed-phase

1

environments (Korolev et al., 2017). Thus, a close evaluation of aerosol-cloud processes is crucial to evaluating weather and climate processes.~~.~~ However, one of the most significant challenges with regard to aerosols is quantifying their impacts on cloud ice formation through serving as ice nucleating particles (INPs) (Boucher et al., 2013). ~~however, c~~Constraining aerosol-cloud impacts in models, specifically when parameterizing INPs in MPC systems, remains a significant challenge due to limited observations (Cziczo et al., 2017; Coluzza et al., 2017; DeMott et al., 2010; Kanji et al., 2017; Korolev et al., 2017). Observations ~~directly in cloudy environments~~directly in-cloud are even more scarce—given the logistical costs and resources required by airborne platforms, caveats associated with aircraft probes and instrumentation, and instrumental artefacts caused by flying through clouds at high speeds (Cziczo et al., 2017)—but are ~~necessary~~ useful~~to assess~~ for assessing ~~the impacts of INPs on MPC microphysics as compared to most surface measurements which are geared towards evaluation of INP sources.

In the absence of conditions with −38 °C and relative humidity with respect to ice above 140%, INPs are required for initiation of tropospheric cloud ice formation (Kanji et al., 2017). Aerosols such as dust and primary biological aerosol particles (PBAPs) are some of the most abundant and efficient INPs found in the atmosphere, respectively (Murray et al., 2012; Hoose and Möhler, 2012; DeMott et al., 1999; Conen et al., 2011; Creamean et al., 2013). PBAPs originating from certain bacteria, pollens, and vegetative detritus are the most efficient INPs known, capable of initiating freezing near −1 °C, while most PBAPs (e.g., fungal spores, algae, and diatoms) tend to nucleate ice at temperatures similar to those of mineral dust (Despres et al., 2012; Murray et al., 2012; Tobo et al., 2014; Hader et al., 2014a; O'Sullivan et al., 2014; Hill et al., 2016; Tesson et al., 2016; Alpert et al., 2011; Knopf et al., 2010; Fröhlich-Nowoisky et al., 2015). In general, previous works collectively indicate that PBAP INPs that nucleate ice at temperatures greater than approximately –10 ˚C are bacterial (Murray et al., 2012; Hu et al., 2018; Hoose and Möhler, 2012; Despres et al., 2012; Frohlich-Nowoisky et al., 2016), but could also be pollen or certain fungal spores (von Blohn et al., 2005; Hoose and Möhler, 2012; O'Sullivan et al., 2016), although the latter two are less likely. Plant bacteria such as *Pseudomonas syringae* are deemed omnipresent in the atmosphere and precipitation (Despres et al., 2012; Stopelli et al., 2017; Morris et al., 2014), and facilitate cloud ice formation up to −1 °C (Despres et al., 2012). While, only a few laboratory-based studies have reported known inorganic or mineral materials ~~that~~ with ice nucleation activity at such temperatures (Ganguly et al., 2018; Atkinson et al., 2013). Mineral and soil dust serving as atmospheric shuttles for organic microbial fragments can be transported thousands of kilometres and serve as effective INPs, even from highly arid regions such as the Sahara (Kellogg and Griffin, 2006). The ~~, yet the exact~~ origin of the ice nucleation germ forming at the warmest temperatures is ~~speculated~~ thought to be due to the ice binding proteins or macromolecules of the biological components in mixed mineral-biological INPs (O'Sullivan et al., 2014; O'Sullivan et al., 2016; Conen and Yakutin, 2018). In general, the previous studies on the climate relevance of PBAPs demonstrate the importance of such INPs at MPC temperatures and precipitation enhancement (Morris et al., 2004; Bergeron, 1935; Christner et al., 2008; Morris et al., 2014; Morris et al., 2017; Stopelli et al., 2014; Frohlich-Nowoisky et al., 2016).

Although biological constituents, from cellular material to in-tact bacteria and spores, are thought to be omnipresent in the atmosphere (Burrows et al., 2009b; Burrows et al., 2009a; Jaenicke, 2005; Jaenicke et al., 2007), modeling studies constraining global emission estimates of biological INPs and PBAPs are very limited, subject to significant hurdles, and often yield conflicting results due to ~~the dearth of~~not having a sufficient set of observations and complexity of atmospheric PBAPs (Hummel et al., 2015; Burrows et al., 2013; Twohy et al., 2016; Frohlich-Nowoisky et al., 2012; Despres et al., 2012; Hoose and Möhler, 2012; Morris et al., 2011). Yet, biological aerosols such as bacteria have been shown to cause significant perturbations in cloud ice in numerical weather prediction models, affording modulations in cloud radiative forcing and precipitation formation (Sahyoun et al., 2017). In addition, measuring and quantifying PBAPs is non-trivial—methodologies for counting, culturing, and nucleic acid sequencing of PBAPs and especially for those which fall in the warm temperature INP regime (i.e., INPs that nucleate ice > −15 °C) are: (1) time

79 and labor intensive, (2) require specific expertise or at times substantial resources, (3) require substantial sample volumes, or (4)

80 are species- or genera-specific or limited to viable microorganisms (Despres et al., 2012). Although such techniques are required

81 to adequately assess the atmospheric microbiome and PBAP sources, a simpler approach could be applied to evaluate and even

82 quantify warm temperature biological INP populations as compared to colder temperature PBAPs or mineral dust.

83 The ~~goal~~ objectives of the study presented here ~~focuses on~~are: (1) to conduct an intercomparison of INP measurements of aerosol,

84 cloud rime, and snow directly ~~in cloudy~~in-cloud ~~environments at the ground~~ and (2) ~~evaluating~~ evaluate different types of INP

85 spectra in a manner such that we can estimate the relative contribution from biological INPs in the warm temperature regime

86 relevant to MPCs. Sampling was conducted at the High -Altitude Research Station Jungfraujoch (JFJ), a unique location for

87 evaluating populations of INPs that affect winter storms in the European Alps, and where MPCs are particularly common

88 (Lohmann et al., 2016). Recent studies at JFJ have provided valuable insight into INP concentrations, sources, and removal

89 processes under a variety of conditions and during various times of the year. Conen et al. (2015) measured INPs at –8 ˚C over the

90 course of a year at JFJ, and found a strong seasonality in such INPs, with two order of magnitude higher concentrations observed

91 during the summer. They also suggested INPs measured at this temperature may be limited most of the year by microphysical

92 processing during transit. Stopelli et al. (2015) verified this removal mechanistic process through INP measurements and isotopic

93 composition of fresh fallen snow at JFJ, concluding that warm temperature INPs ~~(i.e., INPs active at > – 10 ˚C)~~ are rapidly depleted

94 by precipitating clouds at lower elevations. Stopelli et al. (2016) expanded their INP analyses to 2-years of data at JFJ, concluding

95 that a high abundance of INPs at –8 ˚C is to be expected whenever high wind speed coincides with air masses having experienced

96 little or no precipitation prior to sampling, yet a separate study by Stopelli et al. (2017) found that only a small fraction of the INPs

97 were ~~bacterial~~ cultivable cells of *Pseudomonas syringe*. In contrast, Lacher et al. (2018a; 2018b) conducted an interannual synopsis

98 of INP measurements at JFJ and found anthropogenic influence on INP concentrations~~,~~ but only during boundary layer intrusion

99 (BLI) ~~influences~~ and at relatively cold temperatures (i.e., approximately –30 ˚C), and higher INP concentrations during Saharan

100 dust events (SDEs) and marine boundary layer air arriving at JFJ. Eriksen Hammer et al. (2018) characterized ice particle residuals

101 and concluded that silica and aluminosilicates were the most important ice particle residuals at JFJ during the mixed-phase cloud

102 events during Jan – Feb 2017, while carbon-rich particles of possible biological origin were ~~of~~ a minor contribution.

103 Here, we demonstrate how variable sources influence INP populations depending on air mass transport and ~~storm~~ direction, and

104 spectral modality between the rime, snow, and aerosols can help explain the exchange of INPs from air into cloud then into

105 precipitation. Our results expand upon previous studies by evaluating INPs via a combination of aerosol, rime, and snow, and at a

106 temperature range that comprises common biological and mineral INPs.

2 Methods

2.1 Aerosol, cloud rime and snow collection at Jungfraujoch

109 Collocated collection of snow, cloud rime, and aerosol samples for the Ice Nucleation Characterization in the Alps of Switzerland

110 (INCAS) study took place 15 Feb – 11 Mar 2018 in the Sphinx observatory at JFJ (46.55 °N, 7.98 °E; 3580 m above sea level (m

111 a.s.l.); https://www.hfsjg.ch/en/home/). Snow was collected as described by Stopelli et al. (2015) using a Teflon-coated tin (0.1

112 m^2, 8 cm deep) for a duration of 1 – 18 hours, but typically for 1 – 4 hours. Collection quantities and inherent time of collection

113 were dependent upon snowfall rates but additionally on winds blowing snow out of the collection pans. Because of this possibility,

114 we cannot determine actual snowfall rates with certainty. Cloud rime was collected using a slotted plexiglass plate placed vertically

115 during snow sample collection (Lacher et al., 2017; Mignani et al., 2018). Sample collection times were at times longer than the

3

116 duration of in-cloud conditions (see section 2.3) and were dependent on when manually changing the sampling tin and plate was

117 possible. Daily size-resolved aerosol samples were collected using a Davis Rotating-drum Universal-size-cut Monitoring (DRUM)

118 single-jet impactor (DA400, DRUMAir, LLC.) (Cahill et al., 1987; Bukowiecki et al., 2009; Creamean et al., 2018a) as described

119 by Creamean et al. (2018a) from a 1-m long inlet constructed of 6.4-mm inner diameter static-dissipative polyurethane tubing

120 (McMaster-Carr®) leading to outside of the Sphinx and connected to a funnel covered with a loose, perforated plastic bag to

121 prevent rimed ice build-up or blowing snow from clogging the inlet. The DRUM collected aerosol particles at four size ranges

122 (0.15 – 0.34, 0.34 – 1.20, 1.20 – 2.96, and 2.96 – >12 µm in diameter) and sampled at 27.7 L min^{-1} (volumetric flow), equalling

123 39888 total L of air per sample. Such size ranges cover a wide array of aerosols—particularly those that serve as INPs (DeMott et

124 al., 2010; Fridlind et al., 2012; Mason et al., 2016)—while the large volume of air collected promotes collection of rarer, warm

125 temperature biological INPs, but may represent a lower fraction of overall INP concentrations (Mossop and Thorndike, 1966).

126 Samples were deposited onto 20 x 190 mm strips of petrolatum-coated (100%, Vaseline®) perfluoroalkoxy plastic (PFA, 0.05 mm

127 thick) substrate secured onto the rotating drums (20 mm thick, 60 mm in diameter) in each of the four stages at the rate of 7 mm

128 per day (5 mm of sample streaked onto the PFA followed by 2 mm of blank). It is possible local sources of aerosol, such as tobacco

129 smoke or emissions from touristic infrastructure, were collected by the DRUM (Bukowiecki et al., 2016), but did not likely affect

130 the 2.96 – >12 µm particles which we focus on herein. Intervals in which snow, rime, and aerosol were sampled did not fully

131 overlap during a day because conditions were changing often unpredictably between out-of-cloud and in-cloud conditions, the

132 latter with or without precipitation. At the same time we intended to collect enough material from either component for a robust

133 analysis of warm temperature INPs. Consequently, the combined data of a day integrate over a larger air mass, including clouds

134 and cloud-free regions. Comparing data from snow, rime, and aerosol samples still makes sense as long as wind direction and the

135 influence of planetary boundary layer did not change substantially during a day.

136 **2.2 Ice nucleation measurements**

137 All samples were analysed immediately after collection for INPs using a drop freezing cold plate system described by Creamean

138 et al. (2018b; 2018a). Briefly, snow and cloud rime samples were melted into covered 50-mL glass beakers for analysis, resulting

139 in approximately 10 mL of liquid per sample. Samples were manually shaken prior to analysis. Aerosols deposited onto the PFA

140 were prepared for drop freezing by cutting out each daily sample and placing in a 50-mL glass beaker with 2 mL of molecular

141 biology reagent grade water (Sigma-Aldrich®). Beakers were covered and shaken at 500 rpm for 2 hours (Bowers et al., 2009). In

142 between sampling, beakers were cleaned with isopropanol (99.5%), sonicated with double-distilled water for 30 minutes, thenand

143 then heated at 150 °C for 30 minutes.

144 Copper discs (76 mm in diameter, 3.2 mm thick) were prepared by sonicating in double-distilled water for 30 minutes, cleaning

145 with isopropanol, then coated with a thin layer of petrolatum (Tobo, 2016; Bowers et al., 2009). Following sample preparation, a

146 sterile, single-use syringe was used to draw 0.25 mL of the suspension and 100 drops were pipetted onto the petrolatum-coated

147 copper disc, creating an array of ~2.5-µL aliquots. Drops were visually inspected for size; however, it is possible not all drops were

148 the same exact volume, which could lead to a small level of indeterminable undetermined uncertainty. However, previous studies

149 have demonstrated that drop size variability within this range does not significantly impact freezing results (Hader et al., 2014b;

150 Bigg, 1953; Langham and Mason, 1958; Creamean et al., 2018b). The copper disc was then placed on a thermoelectric cold plate

151 (Aldrich®) and covered with a transparent plastic dome. Small holes in the side of the dome and copper disc permitted placement

152 of up to four temperature probes using an Omega™ thermometer/data logger (RDXL4SD; 0.1 °C resolution and accuracy of ±

153 (0.4% + 1 ℃) for the K sensor types used). During the test, the cold plate was cooled at 1 – 10 °C min^{-1} from room temperature

154 until around −35 °C. Control experiments at various cooling rates within this range show very littleno discernible dependency of

drop freezing on cooling rate (Creamean et al., 2018b), akin to previous works (Wright and Petters, 2013; Vali and Stansbury, 1966).

A +0.33 °C correction factor was added to any temperature herein and an uncertainty of 0.15 °C was added to the probe accuracy uncertainty based on DFCP characterization testing presented in Creamean et al. (2018b), to account for the temperature difference between the measurement (i.e., in the plate centre) and actual drop temperature. Frozen drops were detected ~~visually, but~~visually but recorded through custom software. The software records the time, probe temperature, and cooling rate for every second of the test. When a drop is identified as frozen, a button is clicked on the software graphical user interface so that it records that exact time, probe temperature, and cooling rate of that drop in a separate file~~, providing the freezing temperature and cooling rate of each drop frozen~~. The test continue~~dd~~ until all 100 drops were frozen. Each sample was tested three times with 100 new drops for each test. ~~From each test, t~~The fraction frozen ~~and percentage of detected frozen drops were~~was calculated from all detected drops frozen combined from the three tests (typically, > 90% of the drops were detected). The results from the triplicate tests were then binned every 0.5 °C to produce one spectrum per sample. ~~Normalized differential INP spectra were created by a using a combination of calculations. First, c~~Cumulative INP ~~spectra~~concentrations were calculated using the equation ~~posed by~~from Vali (1971):

$$\sout{[INPs(T)]}K(T\sout{L^{-1}}) = -\frac{1}{V_{drop}} \times \ln[1 - f(T)]\ \sout{\frac{\ln N_o - \ln N_u(T)}{V_{drop}}}$$

Where V_{drop} is the average volume of each drop and $f(T)$ is the fraction of drops frozen at temperature T. ~~N_o is the total number of drops, $N_u(T)$ is the number of unfrozen drops at each temperature, and V_{drop} is the average volume of each drop.~~ Normalized differentials of the frequency of freezing events, or df/dT, were calculated finding the difference in $f(T)$ at each temperature bin of 0.5 °C and normalizing to the maximum df/dT value per sample, then smoothed using a moving average. Aerosol cumulative INP concentrations were corrected for the total volume of air per sample ($\sout{INPs}K(T) \times \frac{V_{suspension}}{V_{air}}$) while melted rime/snow residual cumulative INPs were adjusted to the total used during analysis ($K(T)\sout{INPs} \times V_{suspension}$), where $V_{suspension}$ ~~$V_{suspension}$~~ and V_{air} ~~V_{air}~~ represent the total liquid volume analyzed per sample (0.75 mL for the three tests) and total volume of air drawn per sample (39888 L), respectively.

~~Second, differential values were calculated from each 0.5 °C cumulative concentration.~~ Differential INP spectra—which as the name indicates, correspond to the differential of the cumulative spectra (Vali et al., 2015)~~—~~were used early in earlier studies (Vali, 1971; Vali and Stansbury, 1966)~~., h~~owever, ~~s~~Spectra from these previous studies only reached a minimum of –20 ˚C due to the limitations of background artifacts in the water used at that time~~, missing the tail end of what are usually the highest INP concentrations as discussed in more detail below~~. Recent work by Vali (2018) revisits the use of differential spectra, expanding to lower temperatures. We employ the calculation for differential INP concentrations from Vali (2018):

$$k(T) = -\frac{1}{V_{drop} \times \Delta T} \times ln\left(1 - \frac{\Delta N}{N(T)}\right)$$

where N is the number of unfrozen drops and ΔN is the number of freezing events observed between T and $(T - \Delta T)$. ~~Third, d~~Differential concentrations were divided by the maximum concentration per sample (i.e., to normalize)~~. Last, then~~spectra ~~were~~ smoothed using a moving average.

5

2.3 Supporting meteorological and source analysis data

Auxiliary surface meteorological observations, including but not limited to hourly mean air temperature measured 2 m above ground level (a.g.l.) (°C), relative humidity measured 2 m a.g.l. (%), scalar wind speed (m s^{-1}) and direction (degrees), and incoming longwave radiation (W m^{-2}) were acquired from MeteoSwiss (https://gate.meteoswiss.ch/idaweb/). From the longwave measurements, in-cloud conditions were determined by calculating the sky temperature and comparing to air temperature measured at the station, per the methodology of Herrmann et al. (2015) from a 6-year analysis of JFJ observations. There were no in situ measurements of cloud presence or extent. For the current work, each hourly measurement was categorized as out-of-cloud or in-cloud based on such ~~calculations~~calculations and averaged to obtain daily cloud coverage percentage.~~.~~

Radon (^{222}Rn) concentrations have been continuously measured at JFJ since 2009. Details on the detectors themselves and the measurements can be found in Griffiths et al. (2014). Briefly, 30-minute radon concentrations were measured using a dual-flow-loop two-filter radon detector as described by Chambers et al. (2016). Calibrated radon concentrations were converted from activity concentration at ambient conditions to a quantity which is conserved during an air parcel's ascent: activity concentration at standard temperature and pressure (0 °C, 1013 hPa), written as Bq m^{-3} STP (Griffiths et al., 2014). Time periods with ~~boundary layer~~BLI ~~intrusion~~ were classified as radon concentrations > 2 Bq m^{-3} (Griffiths et al., 2014). Particle concentrations from approximately 0.3 to > 20 μm in diameter were measured with a 15-channel optical particle sizer (OPS 3300; TSI, Inc.) at a 1-minute time resolution (Bukowiecki et al., 2016). Due to operational complications, OPS~~C~~ data were not collected prior to 23 Feb during INCAS. Air was drawn through a heated total aerosol inlet (25 °C) which, besides aerosol particles, enables hydrometeors with diameters < 40 ~~μm~~m to enter and to evaporate, at wind speeds of 20 m s^{-1} (Weingartner et al., 1999). SDEs were determined from existing methodology using various aerosol optical properties, but specifically, the Ångström exponent of the single scattering albedo (å$_{SSA}$), which decreases with wavelength during SDEs (Collaud Coen et al., 2004; Bukowiecki et al., 2016). SDEs are automatically detected by the occurrence of negative å$_{SSA}$ that last more than four hours. Based on previous work, m~~M~~ost of the SDEs do not lead to a detectable increase of the 48-h total suspended particulate matter ~~(TSP)~~concentrations at JFJ (Collaud Coen et al., 2004). Additionally, we consider these events probable SDEs, but may have influences from other sources in addition.

Air mass transport analyses were conducted using the HYbrid Single Particle Lagrangian Integrated Trajectory model with the SplitR package for RStudio (https://github.com/rich-iannone/SplitR) (Draxler, 1999; Draxler and Rolph, 2011; Stein et al., 2015). Reanalysis data from the National Centers for Environmental Prediction (NCEP) National Center for Atmospheric Research (NCAR) (2.5° latitude-longitude; 6-hourly; https://www.ready.noaa.gov/gbl_reanalysis.php) were used as the meteorological fields in HYSPLIT simulations. Air mass transport directionality and frontal passages were verified by NCEP/NCAR reanalyses of wind vectors and geopotential height at 600 mb (i.e., approximate pressure at the altitude of JFJ; https://www.esrl.noaa.gov/psd/data/composites/day/). Trajectories were initiated at 10, 500, and 1000 m a.g.l. every 3 hours daily, but only the 500-m trajectories are shown. Trajectories were only simulated for each northwesterly, ~~and~~southeasterly, SDE, and BLI case study day (i.e., Table 1). It is important to note that "northwesterly" is a contribution of north, west, and northwest winds, while "southeasterly" includes south, east, and southeast winds. SDE and BLI days were predominantly (not entirely) southeasterly.

3 Results and discussion

3.1 Directional dichotomy of ~~storm systems~~air masses arriving at JFJ during INCAS

Local surface meteorology was variable at JFJ during INCAS, with air temperatures ranging from –27.5 to –4.8 ˚C (average of –13.7 ˚C)—temperatures relevant to heterogeneous nucleation of cloud ice—and relative humidity ranging from 18 to 100% (Figure 1a~~a~~). All days contained some fraction of in-cloud conditions that varied between 12% and 100%, on average. ~~Wind speed was 6.4 m s⁻¹ on average, with spikes during most storm systems up to 22.8 m s⁻¹ (i.e., wind speed during rime and snow collection; Figure 1b).~~ Due to the topography surrounding JFJ, predominant wind directions were northwest followed by southeast, with the fastest winds recorded originating from the southeast (Figure 2) ~~(Figure 2)~~. Such conditions are typical for JFJ during the winter (Stopelli et al., 2015; Collaud Coen et al., 2011). Out of the entire study, several days were classified as northwesterly (5 days) or southeasterly (2 days) ~~during storm~~ conditions when a combination of aerosol, cloud rime, and snow samples were collected (i.e., a full 24 hours of northwesterly or a full 24 hours of southeasterly winds during snowfall; Table 1), which are herein focused on as the case study days (indicated by the blue and red in Figure 1b, respectively). These days were also deemed days with "storm" conditions since clouds and snow were both present at JFJ. There were 4 days that maintained predominantly southerly wind directions as indicated in green in Figure 1b and Table 1 and were characterized as days influenced by SDEs or BLI as discussed herein. Rime and snow were only collected on one of these days, while remaining SDE or BLI cases had only aerosol collected. Aside from 22 Feb (missing data), the remaining days in the study were characterized as FT and did not exhibit influences from warm temperature INPs (see section 3.2 and 3.3).

Most southeasterly case days (and 06 Mar) apart from the SDE days experienced longer residence times in what was likely the boundary layer (i.e., 1000 m or less) compared to northwesterly cases, which is supported by radon data (Figure 1c). Griffiths et al. (2014) determined that radon concentrations > 2 Bq m⁻³ signify BLI, which in the current work was clearly observed on 23 Feb, 27 Feb, 28 Feb, 06 Mar, and 11 Mar case days, indicating samples collected on these days were likely influenced by continental boundary layer sources. Relatively low radon concentrations were observed the remaining case study days, indicating these samples were predominantly affected by free tropospheric (FT) air and thus, lower aerosol concentrations and/or more distant, including marine, sources. Although OPS data were missing until 23 Feb, source information can be gleaned from the available data. For example, 23 Feb had episodic high concentrations of particles (maximum of 9.6 cm⁻³) towards the beginning of the day coincident with the largest spike in radon, with a steady decrease as time transpired, indicating the boundary layer was an ample source of > 0.3 μm particles. A similar episode with the OPS and radon concentrations was observed 27 – 28 Feb, where the highest concentrations of each were observed during the entire study period. Selected days were subject to diurnal winds (not shown), such as 06 Mar, where boundary layer air reached JFJ and a midday maximum in OPS particle concentrations was observed, indicating lower elevations were the dominant source of aerosol. Although, diurnal variations in aerosol from local sources have been shown to not be common in the winter at JFJ (Baltensperger et al., 1997). In contrast, 11 Mar was exposed to boundary layer air based on radon observations, but particle concentrations were low (average of 0.2 cm⁻³ compared to a study average of 3.0 cm⁻³), signifying that although BLI occurred at JFJ, it was not a substantial source of aerosol. These relationships corroborate the ice nucleation observations, as discussed in detail below.

Extending past local conditions, air mass transport 10 days back in time prior to reaching JFJ on case study days was, as expected, dissimilar between northwesterly (Figure 3) and southeasterly/SDE/BLI (Figure 4) conditions. The main distinctions between northwesterly and southeasterly/SDE/BLI days are: (1) northwesterly days originated from farther west, with some days reaching back to ~~the Canadian Archipelago~~North America, while air masses on southeasterly/SDE/BLI days predominantly hovered over

259   land and ~~occasional~~ oceanic sources closer to Europe, (2) southeasterly/SDE/BLI air masses travelled closer to the surface relative

260   to northwesterly days, ~~especially south and east of JFJ~~ while northwesterly air masses were typically transported from higher

261   altitudes (i.e., more ~~free tropospheric~~FT exposure), and (3) aside from ~~0~~6 Mar (which is discussed in more detail in the following

262   section), northwesterly air masses did not travel over the Mediterranean and northern Africa, whereas the southeasterly/SDE/BLI

263   air masses ~~reaching down to 100 m~~ above JFJ arrived from over such regions within less than 2 days before arriving to JFJ. One

264   obvious inconsistency is that the air mass trajectories on 24 Feb do not indicate transport occurred from Northern Africa even

265   though this day was characterized as an SDE. Collaud Coen et al. (2004) reported that in 71% of all cases they evaluated at JFJ,

266   10-day back-trajectories were able to reveal the source of Saharan dust and that back trajectories cannot always explain SDEs.

267   Boose et al. (2016) reported similar transport pathways for JFJ during multiple consecutive winters and concluded that marine and

268   Saharan dust served as dominant sources of INPs at −33 °C. Reche et al. (2018) also reported similar pathways and sources for

269   bacteria and viruses, but during the summer in southern Spain. ~~Possible SDEs were automatically detected on 24 Feb and 10 Mar~~

270   ~~in the current work, and air mass transport pathways are shown for these days.~~ These disparate sources and transport pathways of

271   air support the variability in the ice nucleation observations as discussed in more detail in the following section.

272   ~~As evidenced by the air mass transport analyses, each southeasterly case day (and 06 Mar) experienced longer residence times in~~

273   ~~what was likely the boundary layer (i.e., 1000 m or less) compared to northwesterly cases, which is supported by [222]Rn data (Figure~~

274   ~~5). Griffiths et al. (2014) determined that radon concentrations > 2 Bq m[-3] signify boundary layer intrusion, which in the current~~

275   ~~work was clearly observed on 23 Feb, 06 Mar, and 11 Mar, indicating samples collected on these days were likely influenced by~~

276   ~~boundary layer sources (planetary and marine). Relatively low radon concentrations were observed the remaining case study days,~~

277   ~~indicating these samples were predominantly affected by free tropospheric air and thus, lower aerosol concentrations and/or more~~

278   ~~distant sources. Although OPC data were missing until 23 Feb, source information can be gleaned from the available data. For~~

279   ~~example, 23 Feb had episodic high concentrations of particles (maximum of 9.6 cm^{-3}) towards the beginning of the day coincident~~

280   ~~with the largest spike in radon, with a steady decrease as time transpired, indicating the boundary layer was an ample source of >~~

281   ~~0.3 μm particles. Although not a case study time period, a similar correlation between the OPC and radon concentrations was~~

282   ~~observed 27 – 28 Feb, where the highest concentrations of each were observed during the entire study time period. Selected days~~

283   ~~were subject to diurnal upslope winds (Figure 1b), such as 6 Mar, where boundary layer air reached JFJ and a midday maximum~~

284   ~~in OPC particle concentrations was observed, indicating lower elevations were the dominant source of aerosol. Although, diurnal~~

285   ~~variations in aerosol from local sources have been shown to not be common in the winter at JFJ (Baltensperger et al., 1997). In~~

286   ~~contrast, 11 Mar was exposed to boundary layer air based on radon observations, but particle concentrations were low (average of~~

287   ~~0.2 cm^{-3} compared to a study average of 3.0 cm^{-3}), signifying that although boundary layer intrusion occurred at JFJ, it was not a~~

288   ~~substantial source of aerosol. These relationships corroborate the ice nucleation observations, as discussed in detail below.~~

289   **3.2 Variability in INP spectra ~~l properties~~ based on ~~storm~~ air mass ~~characteristics~~source**

290   Out of the 25 aerosol, 30 rime, and 39 snow samples collected, 7 aerosol, 19 rime, and 23 snow were collected northwesterly or

291   southeasterly storm case study days, while 4 aerosol, 1 rime, and 2 snow were collected on SDE or BLI days (Table 1). Most

292   ~~m~~Mixed wind direction days were excluded, as sources from both directions would contribute to the daily aerosol sample. Figure

293   ~~5~~6 shows the cumulative ($K(T)$) INP concentrations, normalized differential fraction frozen per 0.5 ºC temperature interval (df/dT),

294   and normalized differential ($k(T)$) INP concentrations from aerosol, snow, and rime samples on the case days ~~compared to air~~

295   ~~temperature, wind speed, and previous measurements at JFJ.~~ The use of df/dT while qualitative and possibly method-specific in

296   terms of modality locations, demonstrates the presence of 1 – 2 INP populations by having a mode in the warm regime (i.e., warm

mode or likely primarily biological) and/or cold regime (i.e., < 15 °C; cold mode or likely a mixture of mineral and biological) (Augustin et al., 2013) and enables us to intercompare between the different types of samples.

In addition to containing higher concentrations of warm temperature INPs, most southeasterly and SDE/BLI samples contained a clear mode in the warm temperature regime compared to northwesterly samples which typically did not contain such a mode in the *df/dT* and *k(T)* spectra. This warm mode, or "bump" at temperatures above approximately –15 ˚C has been observed in a wide range of previous immersion mode ice nucleation studies including but not limited to some of the earliest studies of total aerosol (Vali, 1971), residuals found in hail (Vali and Stansbury, 1966), sea spray aerosol (McCluskey et al., 2017; DeMott et al., 2016), soil samples (Hill et al., 2016), agricultural harvesting emissions (Suski et al., 2018), and in recent reviews of aerosol (Kanji et al., 2017; DeMott et al., 2018) and precipitation (Petters and Wright, 2015) samples. Most previous studies that show spectra with the warm mode typically: (1) report a wide range of freezing temperatures such that it can be observed relative to the steady increase of INPs at colder temperatures or (2) are of samples that include a mixture of biological and mineral or other less efficient INP sources. For example, several previous studies report INP concentrations down to only –15 ˚C (e.g., Conen and Yakutin, 2018; Hara et al., 2016; Kieft, 1988; Schnell and Vali, 1976; Vali et al., 1976; Wex et al., 2015), namely because the goal was to target efficient, warm-temperature biological INPs. However, the warm mode may not be evident in such studies, given it cannot be visualised next to the drastic increase in INPs with temperatures below –15 ˚C (i.e., the cold mode). In contrast, studies conducting INP measurements on known mineral dust samples also are not able to observe the warm mode (e.g., Price et al., 2018; Atkinson et al., 2013; Murray et al., 2012). Together, it is apparent that a mixed biological and mineral (or less efficient biological INPs) sample is needed to assess the modal behaviour in the INP spectra.

Only the largest size range of the aerosol is shown because the remaining size ranges (i.e., < 2.96 µm) were not distinct with respect to wind direction. The fact that size, alone, exhibited directionally-dependent results and that such dependencies were only observed in the coarse mode aerosol indicate: (1) the sources were indeed different between northwesterly, and southeasterly, and SDE/BLI transport—supporting the air mass source analyses—and (2) the coarse mode aerosols were likely from a regional source as opposed to long-range transported thousands of kilometres. This is because gravitational settling typically renders transport of coarse particles inefficient especially within the boundary layer (Creamean et al., 2018a; Jaenicke, 1980). Previous work by Collaud Coen et al. (2018) concludes that the local boundary layer never infrequently influences JFJ in the winter, supporting the fact that regional sources were likely prominent in the current workthe current work (i.e., more FT days (17 of 25 days); Table 1).

Generally, INPs from southeasterly and SDE/BLI days were higher in concentration and more efficient (i.e., were warm temperature INPs that facilitated ice formation > –15 ˚C) than northwesterly samples. Our results are parallel to those by Stopelli et al. (2016), who also observed higher *K(T)* INP concentrations in snow samples collected during southerly conditions at JFJ from Dec 2012 to Oct 2014 (Figure 6a). However, *K(T)*when comparing overlapping temperature ranges from the snow samples during the winter only (Figure 6a), concentrations reported here are were generally higher than those reported by Stopelli et al. (2016), especially for the northwesterly samplesat the highest temperatures. Unlike Stopelli et al. (2016), there was no clear correlation between *K(T)* with air temperature and wind speed in the current work (not shown).

Aside from some of the snow samples, oOnset freezing temperatures (i.e., the highest temperature in which the first drop in each sample froze) were typically higher for samples from the southeast/SDE/BLI samples as compared to the northwest (Figure 6b), indicating influences from more efficient INPssources that produce warm temperature INPs on these days. from the southeast. The temperatures in which 10% (T_{10}) and 50% (T_{50}) of the samples froze were also typically higher for the southeast/SDE/BLI as

9

compared to the northwest samples, especially for the aerosol samples, indicating higher concentrations of more efficient warm temperature INPs. However, a larger (smaller) spread in onset temperatures was observed in samples from the northwest (southeast), suggesting two possibilities: (1) influences were more (less) variable sources from the northwest (southeast), as discussed in more detail in the following section and/or (2) in the case of cloud rime and snow, clouds from the northwest were already depleted with the most efficient INPs due to precipitation prior to arriving at JFJ (i.e., higher transport altitudes which could have been exposed to cloudy conditions as compared to the southeast days which exhibited transport closer to the ground; Figures 3 and 4).

There was no clear correlation between *INP concentrations* with air temperatureR but air temperatures tended to be higher for northwesterly as compared to southeasterly cases. At −25 °C freezing temperatures for the INPs, most northwesterly samples had a range of INP concentrations at higher air temperatures (i.e., > −9 °C), while southeasterly samples exhibited overall higher INP concentrations, but still at a range of air temperatures (Figure 6e). In contrast, there was no correlation or gradient relationship between INP concentrations at any temperature and wind speed (Figure 6f – h), unlike the correlation between wind speed and INPs at −8 °C observed by Stopelli et al. (2016). We also evaluated INP concentrations versus wind speed at −8 °C but did not see any correlation (not shown). Regarding the snow, it is possible that surface processes generate airborne ice particles, which contribute to a snow sample collected at a mountain station (Beck et al., 2018). However, snow that is re-suspended during a snowfall event largely consists of the most recently fallen snow crystals covering wind-exposed surfaces. These particles are unlikely to be different from concurrently falling snow. Hence, their contribution will not change INP abundance or spectral properties of the collected sample. Another matter are hoar frost crystals, which can be very abundant in terms of number, but because of their small size (i.e., < 100 µm (Lloyd et al., 2015)) can only make a minor contribution to the mass of solid precipitation depositing in a tin placed horizontally on a mountain crest. The majority of small crystals will follow the streamlines of air passing over the crest. All that an increased influence of hoar frost particles would do to our observations is to decrease measured differences between snow and rime samples, because additions of hoar frost, a form of rime, would render the collected snow sample a bit more similar to rime.

Figure 7 shows the cumulative and normalized differential INP spectra from the northwesterly and southeasterly case day samples. In addition to containing higher concentrations of warm temperature INPs, more southeasterly samples contained a bimodal distribution relative to the colder and unimodal distributions from northwesterly samples. The warm mode, or "bump" at temperatures above approximately −20 °C has been observed in a wide range of previous immersion mode ice nucleation studies including but not limited to some of the earliest studies of total aerosol (Vali, 1971), residuals found in hail (Vali and Stansbury, 1966), sea spray aerosol (McCluskey et al., 2017; DeMott et al., 2016), soil samples (Hill et al., 2016), agricultural harvesting emissions (Suski et al., 2018), and in recent reviews of aerosol (Kanji et al., 2017; DeMott et al., 2018) and precipitation (Petters and Wright, 2015) samples. Most previous studies that show spectra with the warm mode typically: (1) report a wide range of freezing temperatures such that it can be observed relative to the steady increase of INPs at colder temperatures (i.e., Figure 7, left column) or (2) are of samples that include a mixture of biological and mineral or other less efficient INP sources. For example, several previous studies report INP concentrations down to only −15 °C (e.g., Conen and Yakutin, 2018; Hara et al., 2016; Kieft, 1988; Schnell and Vali, 1976; Vali et al., 1976; Wex et al., 2015), namely because the goal was to target efficient, warm temperature biological INPs. However, the warm mode may not be evident in such studies, given it cannot be visualised next to the drastic increase in INPs with temperatures below −15 °C (i.e., the cold mode). In contrast, studies conducting INP measurements on known mineral dust samples also are not able to observe the warm mode (e.g., Price et al., 2018; Atkinson et al., 2013; Murray

~~et al., 2012). Together, it is apparent that a mixed biological and mineral (or less efficient biological INPs) sample is needed to~~ ~~assess the bimodal behaviour in the INP spectra.~~

3.3 Potential components of INP populations at JFJ

Taking the spectral characteristics in the context of air mass direction and transport can help elucidate the possible sources of INPs at JFJ during INCAS. Qualitative and quantitative evaluation of the warm mode, or likely, the relative contribution of warm temperature biological INPs, to cold mode INPs is transparent when df/dT and $k(T)$ ~~differential INP spectra~~ are calculated (Figure 6e – g~7~). Additionally, normalizing such spectra affords a qualitative comparison of spectra signatures between aerosols and residuals found in cloud rime and snow.

~~Figure 8 shows normalized differential spectral characteristics of daily aerosol, rime, and snow INPs.~~ We offer some possible explanations for the observed variability between the samples. Naturally, the boundary layer more frequently than not contains higher concentrations of warm temperature INPs—and INPs in general—as compared to the free troposphere given the proximity to the sources (e.g., forests, agriculture, vegetation, and the oceans) (Burrows et al., 2013; Despres et al., 2012; Frohlich-Nowoisky et al., 2016; Wilson et al., 2015; Burrows et al., 2009a; Burrows et al., 2009b; Frohlich-Nowoisky et al., 2012; Suski et al., 2018). Although, microorganisms and nanoscale biological fragments are episodically lofted into the free troposphere with mineral dust and transported thousands of kilometres (Creamean et al., 2013; Kellogg and Griffin, 2006).

Air arriving at JFJ on 15 and 16 Feb originated from the farthest away and were not heavily exposed to boundary layer air, as evidenced by the air mass trajectory analysis (Figure 3) and radon (Figure 1c~5~), indicating long-range transport in the free troposphere. This could explain why the warm mode (and higher T_{10} and T_{50}) was observed for ~~in~~ the rime and snow, but not the aerosol—the aerosol had sufficient time to nucleate ice during free tropospheric transport and especially the warm temperature INPs that would likely become depleted in-cloud first (Stopelli et al., 2015), assuming the clouds formed along the air mass transport pathways~~, as also supported by the higher INP concentrations in most of the rime and snow compared to the aerosol in Figure 6b~~. Cloud fraction was relatively low (12.5 to 25%), but air temperatures were relatively high (–8.4 to –7.1 ˚C), suggesting conditions were amenable for long-range transported warm temperature INPs to nucleate cloud ice. However, from the available data, we cannot determine with certainty if the local conditions were the same as those when nucleation initially occurred. For 19 and 20 Feb, air temperature was ~~very~~ cold (–16.4 and –19.6 ˚C, respectively) cloud fraction was high (92 and 54%, respectively), and all samples ~~remained unimodal~~ did not contain a warm mode~~(i.e., only containing the cold mode)~~. One possible explanation is that any warm temperature INPs that were present in the clouds had already snowed out prior to reaching the sampling location, as observed by Stopelli et al. (2015) at JFJ. Although, given the low radon concentrations and erratic transport pathways, it is possible such air masses did not contain a relatively large concentrations of warm temperature INPs due to deficient exchange with the boundary layer. It was not until the southeasterly cases that the aerosol samples exhibited ~~bimodal~~ a warm mode~~characteristics~~ ~~(i.e., contained both the warm and cold modes)~~. Specifically, on 23 Feb local winds shifted to southeasterly (147 degrees on average) and air masses arrived from over the eastern Alps, Eastern Europe, Scandinavia, and earlier on in time, the Atlantic Ocean. Thus, these samples were predominantly influenced by the continental (mostly over remote regions) and marine boundary layers ~~(Figures 4 and 5)~~, where sources of warm temperature INPs are more abundant (Frohlich-Nowoisky et al., 2016).

The northwesterly case of 0~0~6 Mar is somewhat interesting in that the local wind direction was clearly from the northwest, but air mass source analyses show brief transport in the boundary layer (radon) from the south, when looking farther back in time, traveling over the Mediterranean and North Africa. The aerosol sample had ~~the third highest~~a high onset temperature for INPs relative to

other northwest samples (Figure 6b) and snow samples exhibited ~~bimodality~~ a warm mode (Figure ~~6g~~ 8e). It is the only one of the northwesterly case samples that encountered boundary layer exposure according to the radon observations. Combined, these results suggest a somewhat mixed-source sample, and that 06 Mar may not be directly parallel to the other northwesterly cases. Transitioning back to a southeasterly case on 11 Mar, only the rime and snow unveiled ~~bimodal behaviour~~ a warm mode from air transported from similar regions as the 06 Mar sample. ~~However, transport on 11 Mar was more directly from the south over the Mediterranean and North Africa, indicating less time for removal of the INPs during transport.~~ Additionally, OP~~SC~~ concentrations were very low (Figure ~~5~~1c). These results suggest the aerosols already nucleated cloud ice prior to reaching JFJ on 11 Mar (i.e., low ambient aerosol), ~~which is supported by the 10 Mar sampling~~ where the aerosol ~~was bimodal~~did not contain a warm mode, but rime and snow did. ~~rime was unimodal, and snow was bimodal, but the warm mode resided at a relatively cold temperature (–16.5 °C).~~

~~Two other days without snowfall support the conclusion that southeasterly air mass transport introduces warm temperature INPs to JFJ.~~When evaluating the SDE and BLI days, there is a bit of variability. On 24 Feb, clouds were present at JFJ (a cloud fraction of 37.5%), but riming was insufficient to collect ~~a sufficient~~enough quantity for INP analysis and no snowfall occurred. Interestingly, the warm mode was the ~~maximum~~ second highest for the aerosol sampl~~e – normally, the cold mode has the highest normalized value –~~e and it did not contain a cold mode (for *df/dT*), indicating a ~~larger~~ relatively large contribution of warm temperature INPs as compared to the total INP population. Air mass transport was very similar to 23 Feb signifying similar INP sources even though this day was characterized as an SDE, but it is probable that a slightly warmer (–6.0 as compared to –9.8 °C air temperature), drier (79 versus 89% relative humidity), and higher pressure (649 versus 645 mb) postfrontal system moved over JFJ on 24 Feb, inhibiting removal of warm temperature INPs during transport relative to the day prior (corroborated by reanalysis from NCEP/NCAR of geopotential height at 600 mb). The ~~second~~ BLI case ~~of~~ , 28 Feb ~~(not shown)~~ was very similar to 24 Feb in that: (1) only an aerosol sample was collected and (2) the warm mode was the maximum mode for *df/dT*. As compared to 27 Feb where a warm mode was not observed, 28 Feb was warmer (−20.0 as compared to −26.2 °C), drier (52 versus 62%), higher pressure (635 versus 630 mb), and had a warmer onset temperature (–6.8 versus –14.8 °C). Wind direction was slightly different: southeasterly (153 degrees) on 27 Feb as compared to southwesterly on 28 Feb (221 degrees). However, conditions were cloudier than the 23 – 24 Feb coupling and completely cloudy on 27 Feb (100 and 66.7% cloud fraction on 27 Feb and 28 Feb, respectively). Additionally, radon and OP~~SC~~ concentrations were the highest on 27 – 28 Feb as compared to the rest of the days during INCAS (Figure 1c~~5~~). Combined, these results suggest a very local, boundary layer source of INPs started on 27 Feb, but were quickly depleted in the very cloudy conditions. Once clouds started to clear and a shift in frontal characteristics occurred, a similar source of very efficient warm temperature INPs affected JFJ but were able to be observed in the aerosol.

4 Conclusions and broader implications

Aerosol, cloud rime, and snow samples were collected at the High -Altitude Research Station Jungfraujoch during the INCAS field campaign in Feb and Mar 2018. The objectives of the study were to assess variability in wintertime INP sources found in cloudy environments and evaluate relationships between INPs found in the different sample materials. To directly compare air to liquid samples, characteristics of normalized differential fraction frozen and INP spectra were compared in the context of cumulative INP spectra statistics, air mass transport and exposure to boundary layer or free tropospheric conditions, and local meteorology. Distinction between northwesterly and southeasterly conditions yielded variable results regarding INP efficiency and concentrations, biological versus non-biological sources, and meteorological conditions at the sampling location. In general, cumulative INP concentrations were 3 to 20 times higher for all sample types when sources from the southeast infiltrated JFJ,

while the ~~modality of the~~ INP spectra of the aerosol ~~was bimodal~~ contained a warm mode ~~for aerosol~~ but the presence of a warm mode was variable for the rime and snow depending on meteorological context.

In general, comprehensive measurements of INPs from aerosol, and rime and snow when possible, affords useful information to compare and explain exchange between aerosols, clouds, and precipitation in the context of local and regional scale meteorology and transport conditions. Assessment of different INP spectral types, modality, and spectra statistics adds another dimension for qualitative and semi-quantitative intercomparison of sampling days and evaluation of associations between aerosol, cloud, and precipitation sampling. Extending INP analyses past reporting cumulative concentrations affords more detailed information on the population of INPs and enables comparison between samples from aerosols, clouds, precipitation, and beyond (e.g., seawater, soil, etc.). Using auxiliary measurements and air mass simulations, in addition to context provided by previous work at JFJ, we have addressed possible sources for INCAS. However, more detailed source apportionment work should be imminent to comprehensively characterize INP sources based on spectral features. Future studies should ideally use such statistical analyses in tandem with focused chemical and biological characterization assessments to provide direct linkages between INP spectral properties and sources. Such investigations could yield valuable information on INP sources, and aerosol-cloud-precipitation interactions, which could then be used to improve process-level model parameterizations of such interactions by rendering quantitative information on INP source, efficiency, and abundance. Improving understanding of aerosol impacts on clouds and precipitation will ultimately significantly enhance understanding of the earth system with respect to cloud effects on the surface energy and water budgets to address future concerns of climate change and water availability.

Author contributions

JMC collected the samples, conducted the DFA sample analysis, conducted data analysis, and wrote the manuscript. CM and FC also contributed to collecting rime and snow samples. JMC, CM, and FC designed the experiments. NB provided quality controlled OPS data. CM, NB, and FC helped with manuscript feedback and revision prior to submission.

Acknowledgements

References

Albrecht, B. A.: Aerosols, Cloud Microphysics, and Fractional Cloudiness, Science, 245, 1227-1230, 10.1126/science.245.4923.1227, 1989.

Alpert, P. A., Aller, J. Y., and Knopf, D. A.: Ice nucleation from aqueous NaCl droplets with and without marine diatoms, Atmos. Chem. Phys., 11, 5539-5555, 10.5194/acp-11-5539-2011, 2011.

Atkinson, J. D., Murray, B. J., Woodhouse, M. T., Whale, T. F., Baustian, K. J., Carslaw, K. S., Dobbie, S., O'Sullivan, D., and Malkin, T. L.: The importance of feldspar for ice nucleation by mineral dust in mixed-phase clouds, Nature, 498, 355-358, 10.1038/nature12278, 2013.

Augustin, S., Wex, H., Niedermeier, D., Pummer, B., Grothe, H., Hartmann, S., Tomsche, L., Clauss, T., Voigtländer, J., Ignatius, K., and Stratmann, F.: Immersion freezing of birch pollen washing water, Atmos. Chem. Phys., 13, 10989-11003, 10.5194/acp-13-10989-2013, 2013.

Baltensperger, U., Gäggeler, H. W., Jost, D. T., Lugauer, M., Schwikowski, M., Weingartner, E., and Seibert, P.: Aerosol climatology at the high-alpine site Jungfraujoch, Switzerland, Journal of Geophysical Research: Atmospheres, 102, 19707-19715, doi:10.1029/97JD00928, 1997.

Beck, A., Henneberger, J., Fugal, J. P., David, R. O., Lacher, L., and Lohmann, U.: Impact of surface and near-surface processes on ice crystal concentrations measured at mountain-top research stations, Atmos Chem Phys, 18, 8909-8927, 10.5194/acp-18-8909-2018, 2018.

Bergeron, T.: On the physics of cloud and precipitation, 5th Assembly of the U.G.G.I., Paul Dupont, Paris, 1935.

Bigg, E. K.: The Supercooling of Water, P Phys Soc Lond B, 66, 688-694, Doi 10.1088/0370-1301/66/8/309, 1953.

Boose, Y., Sierau, B., Garcia, M. I., Rodriguez, S., Alastuey, A., Linke, C., Schnaiter, M., Kupiszewski, P., Kanji, Z. A., and Lohmann, U.: Ice nucleating particles in the Saharan Air Layer, Atmos. Chem. Phys., 16, 9067-9087, 2016.

Boucher, O., Randall, D., Artaxo, P., Bretherton, C., Feingold, G., Forster, P., Kerminen, V.-M., Kondo, Y., Liao, H., Lohmann, U., Rasch, P., Satheesh, S. K., Sherwood, S., Stevens, B., and Zhang, X. Y.: Clouds and Aerosols, in: Climate Change 2013: The Physical Science Basis. Contribution of Working Group I to the Fifth Assessment Report of the Intergovernmental Panel on Climate Change, edited by: Stocker, T. F., Qin, D., Plattner, G.-K., Tignor, M., Allen, S. K., Boschung, J., Nauels, A., Xia, Y., Bex, V., and Midgley, P. M., Cambridge University Press, Cambridge, United Kingdom and New York, NY, USA, 571–658, 2013.

Bowers, R. M., Lauber, C. L., Wiedinmyer, C., Hamady, M., Hallar, A. G., Fall, R., Knight, R., and Fierer, N.: Characterization of Airborne Microbial Communities at a High-Elevation Site and Their Potential To Act as Atmospheric Ice Nuclei, Applied and Environmental Microbiology, 75, 5121-5130, 10.1128/Aem.00447-09, 2009.

Bukowiecki, N., Richard, A., Furger, M., Weingartner, E., Aguirre, M., Huthwelker, T., Lienemann, P., Gehrig, R., and Baltensperger, U.: Deposition Uniformity and Particle Size Distribution of Ambient Aerosol Collected with a Rotating Drum Impactor, Aerosol Science and Technology, 43, 891-901, 10.1080/02786820903002431, 2009.

Bukowiecki, N., Weingartner, E., Gysel, M., Coen, M. C., Zieger, P., Herrmann, E., Steinbacher, M., Gäggeler, H. W., and Baltensperger, U.: A Review of More than 20 Years of Aerosol Observation at the High Altitude Research Station Jungfraujoch, Switzerland (3580 m asl), Aerosol and Air Quality Research, 16, 764-788, 10.4209/aaqr.2015.05.0305, 2016.

Burrows, S. M., Butler, T., Jockel, P., Tost, H., Kerkweg, A., Poschl, U., and Lawrence, M. G.: Bacteria in the global atmosphere - Part 2: Modeling of emissions and transport between different ecosystems, Atmos Chem Phys, 9, 9281-9297, DOI 10.5194/acp-9-9281-2009, 2009a.

Burrows, S. M., Elbert, W., Lawrence, M. G., and Poschl, U.: Bacteria in the global atmosphere - Part 1: Review and synthesis of literature data for different ecosystems, Atmos Chem Phys, 9, 9263-9280, DOI 10.5194/acp-9-9263-2009, 2009b.

Burrows, S. M., Hoose, C., Poschl, U., and Lawrence, M. G.: Ice nuclei in marine air: biogenic particles or dust?, Atmos Chem Phys, 13, 245-267, 10.5194/acp-13-245-2013, 2013.

Cahill, T. A., Feeney, P. J., and Eldred, R. A.: Size Time Composition Profile of Aerosols Using the Drum Sampler, Nucl Instrum Meth B, 22, 344-348, Doi 10.1016/0168-583x(87)90355-7, 1987.

Chambers, S. D., Williams, A. G., Conen, F., Griffiths, A. D., Reimann, S., Steinbacher, M., Krummel, P. B., Steele, L. P., van der Schoot, M. V., Galbally, I. E., Molloy, S. B., and Barnes, J. E.: Towards a Universal "Baseline" Characterisation of Air Masses for High- and Low-Altitude Observing Stations Using Radon-222, Aerosol and Air Quality Research, 16, 885-899, 10.4209/aaqr.2015.06.0391, 2016.

Christner, B. C., Morris, C. E., Foreman, C. M., Cai, R. M., and Sands, D. C.: Ubiquity of biological ice nucleators in snowfall, Science, 319, 1214-1214, 10.1126/science.1149757, 2008.

Collaud Coen, M., Weingartner, E., Schaub, D., Hueglin, C., Corrigan, C., Henning, S., Schwikowski, M., and Baltensperger, U.: Saharan dust events at the Jungfraujoch: detection by wavelength dependence of the single scattering albedo and first climatology analysis, Atmos. Chem. Phys., 4, 2465-2480, 2004.

Collaud Coen, M., Weingartner, E., Furger, M., Nyeki, S., Prevot, A. S. H., Steinbacher, M., and Baltensperger, U.: Aerosol climatology and planetary boundary influence at the Jungfraujoch analyzed by synoptic weather types, Atmos Chem Phys, 11, 5931-5944, 10.5194/acp-11-5931-2011, 2011.

Collaud Coen, M., Andrews, E., Aliaga, D., Andrade, M., Angelov, H., Bukowiecki, N., Ealo, M., Fialho, P., Flentje, H., Hallar, A. G., Hooda, R., Kalapov, I., Krejci, R., Lin, N.-H., Marinoni, A., Ming, J., Nguyen, N. A., Pandolfi, M., Pont, V., Ries, L., Rodriguez, S., Schauer, G., Sellegri, K., Sharma, S., Sun, J., Tunved, P., Velasquez, P., and Ruffieux, D.: Identification of topographic features influencing aerosol observations at high altitude stations, Atmos. Chem. Phys., 18, 12289-12313, 2018.

Coluzza, I., Creamean, J., Rossi, M., Wex, H., Alpert, P., Bianco, V., Boose, Y., Dellago, C., Felgitsch, L., Fröhlich-Nowoisky, J., Herrmann, H., Jungblut, S., Kanji, Z., Menzl, G., Moffett, B., Moritz, C., Mutzel, A., Pöschl, U., Schauperl, M., Scheel, J., Stopelli, E., Stratmann, F., Grothe, H., and Schmale, D.: Perspectives on the Future of Ice Nucleation Research: Research Needs and Unanswered Questions Identified from Two International Workshops, Atmosphere, 8, 138, 2017.

Conen, F., Morris, C. E., Leifeld, J., Yakutin, M. V., and Alewell, C.: Biological residues define the ice nucleation properties of soil dust, Atmos. Chem. Phys., 11, 9643-9648, 10.5194/acp-11-9643-2011, 2011.

Conen, F., Rodriguez, S., Huglin, C., Henne, S., Herrmann, E., Bukowiecki, N., and Alewell, C.: Atmospheric ice nuclei at the high-altitude observatory Jungfraujoch, Switzerland, Tellus B, 67, 10.3402/tellusb.v67.25014, 2015.

Conen, F., and Yakutin, M. V.: Soils rich in biological ice-nucleating particles abound in ice-nucleating macromolecules likely produced by fungi, Biogeosciences, 15, 4381-4385, 10.5194/bg-15-4381-2018, 2018.

Creamean, J. M., Suski, K. J., Rosenfeld, D., Cazorla, A., DeMott, P. J., Sullivan, R. C., White, A. B., Ralph, F. M., Minnis, P., Comstock, J. M., Tomlinson, J. M., and Prather, K. A.: Dust and Biological Aerosols from the Sahara and Asia Influence Precipitation in the Western U.S., Science, 339, 1572-1578, DOI 10.1126/science.1227279, 2013.

Creamean, J. M., Kirpes, R. M., Pratt, K. A., Spada, N. S., Maahn, M., de Boer, G., Schnell, R. C., and China, S.: Marine and terrestrial influences on ice nucleating particles during continuous springtime measurements in an Arctic oilfield location, Atmos Chem Phys, 18, 1-20, https://doi.org/10.5194/acp-18-1-2018, 2018a.

Creamean, J. M., Primm, K. M., Tolbert, M. A., Hall, E. G., Wendell, J., Jordan, A., Sheridan, P. J., Smith, J., and Schnell, R. C.: HOVERCAT: A novel aerial system for evaluation of aerosol-cloud interactions, Atmos. Meas. Tech., submitted, 2018b.

Cziczo, D. J., Ladino, L., Boose, Y., Kanji, Z. A., Kupiszewski, P., Lance, S., Mertes, S., and Wex, H.: Measurements of Ice Nucleating Particles and Ice Residuals, Meteorological Monographs, 58, 8.1-8.13, 10.1175/amsmonographs-d-16-0008.1, 2017.

DeMott, P. J., Chen, Y., Kreidenweis, S. M., Rogers, D. C., and Sherman, D. E.: Ice formation by black carbon particles, Geophys Res Lett, 26, 2429-2432, Doi 10.1029/1999gl900580, 1999.

DeMott, P. J., Prenni, A. J., Liu, X., Kreidenweis, S. M., Petters, M. D., Twohy, C. H., Richardson, M. S., Eidhammer, T., and Rogers, D. C.: Predicting global atmospheric ice nuclei distributions and their impacts on climate, P Natl Acad Sci USA, 107, 11217-11222, 10.1073/pnas.0910818107, 2010.

DeMott, P. J., Hill, T. C. J., McCluskey, C. S., Prather, K. A., Collins, D. B., Sullivan, R. C., Ruppel, M. J., Mason, R. H., Irish, V. E., Lee, T., Hwang, C. Y., Rhee, T. S., Snider, J. R., McMeeking, G. R., Dhaniyala, S., Lewis, E. R., Wentzell, J. J. B., Abbatt, J., Lee, C., Sultana, C. M., Ault, A. P., Axson, J. L., Martinez, M. D., Venero, I., Santos-Figueroa, G., Stokes, M. D., Deane, G. B., Mayol-Bracero, O. L., Grassian, V. H., Bertram, T. H., Bertram, A. K., Moffett, B. F., and Franc, G. D.: Sea spray aerosol as a unique source of ice nucleating particles, P Natl Acad Sci USA, 113, 5797-5803, 10.1073/pnas.1514034112, 2016.

DeMott, P. J., Möhler, O., Cziczo, D. J., Hiranuma, N., Petters, M. D., Petters, S. S., Belosi, F., Bingemer, H. G., Brooks, S. D., Budke, C., Burkert-Kohn, M., Collier, K. N., Danielczok, A., Eppers, O., Felgitsch, L., Garimella, S., Grothe, H., Herenz, P., Hill, T. C. J., Höhler, K., Kanji, Z. A., Kiselev, A., Koop, T., Kristensen, T. B., Krüger, K., Kulkarni, G., Levin, E. J. T., Murray, B. J., Nicosia, A., D., O. S., A., P., J., P. M., C., P. H., Reicher, N., Rothenberg, D. A., Rudich, Y., Santachiara, G., Schiebel, T., Schrod, J., Seifried, T. M., Stratmann, F., Sullivan, R. C., Suski, K. J., Szakáll, M., Taylor, H. P., Ullrich, R., Vergara-Temprado, J., Wagner, R., Whale, T. F., Weber, D., Welti, A., Wilson, T. W., Wolf, M. J., and Zenker, J.: The Fifth International Workshop on Ice Nucleation phase 2 (FIN-02): Laboratory intercomparison of ice nucleation measurements, Atmos. Meas. Tech., in review, https://doi.org/10.5194/amt-2018-191, 2018.

Despres, V. R., Huffman, J. A., Burrows, S. M., Hoose, C., Safatov, A. S., Buryak, G., Frohlich-Nowoisky, J., Elbert, W., Andreae, M. O., Poschl, U., and Jaenicke, R.: Primary biological aerosol particles in the atmosphere: a review, Tellus B, 64, 10.3402/tellusb.v64i0.15598, 2012.

Draxler, R. R.: HYSPLIT4 user's guide, NOAA Air Resources Laboratory, Silver Spring, MD., 1999.

Draxler, R. R., and Rolph, G.: HYSPLIT (HYbrid Single-Particle Lagrangian Integrated Trajectory) Model access via NOAA ARL READY website (http://ready.arl.noaa.gov/hysplit.php), NOAA Air Resources Laboratory, Silver Spring, MD, 2011.

Eriksen Hammer, S., Mertes, S., Schneider, J., Ebert, M., Kandler, K., and Weinbruch, S.: Composition of ice particle residuals in mixed-phase clouds at Jungfraujoch (Switzerland): enrichment and depletion of particle groups relative to total aerosol, Atmos. Chem. Phys., 18, 13987-14003, 2018.

Fridlind, A. M., Diedenhoven, B. v., Ackerman, A. S., Avramov, A., Mrowiec, A., Morrison, H., Zuidema, P., and Shupe, M. D.: A FIRE-ACE/SHEBA Case Study of Mixed-Phase Arctic Boundary Layer Clouds: Entrainment Rate Limitations on Rapid Primary Ice Nucleation Processes, Journal of the Atmospheric Sciences, 69, 365-389, 10.1175/jas-d-11-052.1, 2012.

598 Frohlich-Nowoisky, J., Burrows, S. M., Xie, Z., Engling, G., Solomon, P. A., Fraser, M. P., Mayol-Bracero, O. L., Artaxo, P.,
599   Begerow, D., Conrad, R., Andreae, M. O., Despres, V. R., and Poschl, U.: Biogeography in the air: fungal diversity over
600   land and oceans, Biogeosciences, 9, 1125-1136, 10.5194/bg-9-1125-2012, 2012.
601 Frohlich-Nowoisky, J., Kampf, C. J., Weber, B., Huffman, J. A., Pohlker, C., Andreae, M. O., Lang-Yona, N., Burrows, S. M.,
602   Gunthe, S. S., Elbert, W., Su, H., Hoor, P., Thines, E., Hoffmann, T., Despres, V. R., and Poschl, U.: Bioaerosols in the
603   Earth system: Climate, health, and ecosystem interactions, Atmos Res, 182, 346-376, 10.1016/j.atmosres.2016.07.018,
604   2016.
605 Fröhlich-Nowoisky, J., Hill, T. C. J., Pummer, B. G., Yordanova, P., Franc, G. D., and Pöschl, U.: Ice nucleation activity in the
606   widespread soil fungus <i>Mortierella alpina</i>, Biogeosciences, 12, 1057-1071, 10.5194/bg-12-1057-2015, 2015.
607 Ganguly, M., Dib, S., and Ariya, P. A.: Purely Inorganic Highly Efficient Ice Nucleating Particle, ACS Omega, 3, 3384-3395,
608   10.1021/acsomega.7b01830, 2018.
609 Griffiths, A. D., Conen, F., Weingartner, E., Zimmermann, L., Chambers, S. D., Williams, A. G., and Steinbacher, M.: Surface-
610   to-mountaintop transport characterised by radon observations at the Jungfraujoch, Atmos Chem Phys, 14, 12763-12779,
611   10.5194/acp-14-12763-2014, 2014.
612 Hader, J. D., Wright, T. P., and Petters, M. D.: Contribution of pollen to atmospheric ice nuclei concentrations, Atmos. Chem.
613   Phys., 14, 5433-5449, 10.5194/acp-14-5433-2014, 2014a.
614 Hader, J. D., Wright, T. P., and Petters, M. D.: Contribution of pollen to atmospheric ice nuclei concentrations, Atmos Chem Phys,
615   14, 5433-5449, 10.5194/acp-14-5433-2014, 2014b.
616 Hara, K., Maki, T., Kakikawa, M., Kobayashi, F., and Matsuki, A.: Effects of different temperature treatments on biological ice
617   nuclei in snow samples, Atmos Environ, 140, 415-419, 10.1016/j.atmosenv.2016.06.011, 2016.
618 Herrmann, E., Weingartner, E., Henne, S., Vuilleumier, L., Bukowiecki, N., Steinbacher, M., Conen, F., Coen, M. C., Hammer,
619   E., Juranyi, Z., Baltensperger, U., and Gysel, M.: Analysis of long-term aerosol size distribution data from Jungfraujoch
620   with emphasis on free tropospheric conditions, cloud influence, and air mass transport, J Geophys Res-Atmos, 120, 9459-
621   9480, 10.1002/2015jd023660, 2015.
622 Hill, T. C. J., DeMott, P. J., Tobo, Y., Fröhlich-Nowoisky, J., Moffett, B. F., Franc, G. D., and Kreidenweis, S. M.: Sources of
623   organic ice nucleating particles in soils, Atmos. Chem. Phys., 16, 7195-7211, 10.5194/acp-16-7195-2016, 2016.
624 Hoose, C., and Möhler, O.: Heterogeneous ice nucleation on atmospheric aerosols: a review of results from laboratory experiments,
625   Atmos. Chem. Phys., 12, 9817-9854, 10.5194/acp-12-9817-2012, 2012.
626 Hu, W., Niu, H. Y., Murata, K., Wu, Z. J., Hu, M., Kojima, T., and Zhang, D. Z.: Bacteria in atmospheric waters: Detection,
627   characteristics and implications, Atmos Environ, 179, 201-221, 10.1016/j.atmosenv.2018.02.026, 2018.
628 Hummel, M., Hoose, C., Gallagher, M., Healy, D. A., Huffman, J. A., O'Connor, D., Poschl, U., Pohlker, C., Robinson, N. H.,
629   Schnaiter, M., Sodeau, J. R., Stengel, M., Toprak, E., and Vogel, H.: Regional-scale simulations of fungal spore aerosols
630   using an emission parameterization adapted to local measurements of fluorescent biological aerosol particles, Atmos
631   Chem Phys, 15, 6127-6146, 10.5194/acp-15-6127-2015, 2015.
632 Jaenicke, R.: Atmospheric aerosols and global climate, Journal of Aerosol Science, 11, 577-588, https://doi.org/10.1016/0021-
633   8502(80)90131-7, 1980.
634 Jaenicke, R.: Abundance of Cellular Material and Proteins in the Atmosphere, Science, 308, 73-73, 10.1126/science.1106335,
635   2005.
636 Jaenicke, R., Matthias-Maser, S., and Gruber, S.: Omnipresence of biological material in the atmosphere, Environmental
637   Chemistry, 4, 217-220, https://doi.org/10.1071/EN07021, 2007.
638 Kanji, Z. A., Ladino, L. A., Wex, H., Boose, Y., Burkert-Kohn, M., Cziczo, D. J., and Krämer, M.: Overview of Ice Nucleating
639   Particles, Meteorological Monographs, 58, 1.1-1.33, 10.1175/amsmonographs-d-16-0006.1, 2017.
640 Kellogg, C. A., and Griffin, D. W.: Aerobiology and the global transport of desert dust, Trends Ecol Evol, 21, 638-644,
641   10.1016/j.tree.2006.07.004, 2006.
642 Kieft, T. L.: Ice Nucleation Activity in Lichens, Applied and Environmental Microbiology, 54, 1678-1681, 1988.
643 Knopf, D. A., Alpert, P. A., Wang, B., and Aller, J. Y.: Stimulation of ice nucleation by marine diatoms, Nature Geoscience, 4,
644   88, 10.1038/ngeo1037, 2010.
645 Korolev, A., McFarquhar, G., Field, P. R., Franklin, C., Lawson, P., Wang, Z., Williams, E., Abel, S. J., Axisa, D., Borrmann, S.,
646   Crosier, J., Fugal, J., Krämer, M., Lohmann, U., Schlenczek, O., Schnaiter, M., and Wendisch, M.: Mixed-Phase Clouds:
647   Progress and Challenges, Meteorological Monographs, 58, 5.1-5.50, 10.1175/amsmonographs-d-17-0001.1, 2017.
648 Lacher, L., Lohmann, U., Boose, Y., Zipori, A., Herrmann, E., Bukowiecki, N., Steinbacher, M., and Kanji, Z. A.: The Horizontal
649   Ice Nucleation Chamber (HINC): INP measurements at conditions relevant for mixed-phase clouds at the High Altitude
650   Research Station Jungfraujoch, Atmos. Chem. Phys., 17, 15199–15224, https://doi.org/10.5194/acp-17-15199-2017,
651   2017.
652 Lacher, L., DeMott, P. J., Levin, E. J. T., Suski, K. J., Boose, Y., Zipori, A., Herrmann, E., Bukowiecki, N., Steinbacher, M., Gute,
653   E., Abbatt, J. P. D., Lohmann, U., and Kanji, Z. A.: Background Free-Tropospheric Ice Nucleating Particle Concentrations
654   at Mixed-Phase Cloud Conditions, Journal of Geophysical Research: Atmospheres, 123, doi:10.1029/2018JD028338,
655   2018a.

Lacher, L., Steinbacher, M., Bukowiecki, N., Herrmann, E., Zipori, A., and Kanji, Z. A.: Impact of Air Mass Conditions and Aerosol Properties on Ice Nucleating Particle Concentrations at the High Altitude Research Station Jungfraujoch, Atmosphere, 9, 2018b.

Langham, E. J., and Mason, B. J.: The Heterogeneous and Homogeneous Nucleation of Supercooled Water, Proc R Soc Lon Ser-A, 247, 493-&, DOI 10.1098/rspa.1958.0207, 1958.

Lloyd, G., Choularton, T. W., Bower, K. N., Gallagher, M. W., Connolly, P. J., Flynn, M., Farrington, R., Crosier, J., Schlenczek, O., Fugal, J., and Henneberger, J.: The origins of ice crystals measured in mixed-phase clouds at the high-alpine site Jungfraujoch, Atmos Chem Phys, 15, 12953-12969, 10.5194/acp-15-12953-2015, 2015.

Lohmann, U., Henneberger, J., Henneberg, O., Fugal, J. P., Bühl, J., and Kanji, Z. A.: Persistence of orographic mixed-phase clouds, Geophys Res Lett, 43, 10,512-510,519, doi:10.1002/2016GL071036, 2016.

Mason, R. H., Si, M., Chou, C., Irish, V. E., Dickie, R., Elizondo, P., Wong, R., Brintnell, M., Elsasser, M., Lassar, W. M., Pierce, K. M., Leaitch, W. R., MacDonald, A. M., Platt, A., Toom-Sauntry, D., Sarda-Esteve, R., Schiller, C. L., Suski, K. J., Hill, T. C. J., Abbatt, J. P. D., Huffman, J. A., DeMott, P. J., and Bertram, A. K.: Size-resolved measurements of ice-nucleating particles at six locations in North America and one in Europe, Atmos Chem Phys, 16, 1637-1651, 10.5194/acp-16-1637-2016, 2016.

McCluskey, C. S., Hill, T. C. J., Malfatti, F., Sultana, C. M., Lee, C., Santander, M. V., Beall, C. M., Moore, K. A., Cornwell, G. C., Collins, D. B., Prather, K. A., Jayarathne, T., Stone, E. A., Azam, F., Kreidenweis, S. M., and DeMott, P. J.: A Dynamic Link between Ice Nucleating Particles Released in Nascent Sea Spray Aerosol and Oceanic Biological Activity during Two Mesocosm Experiments, Journal of the Atmospheric Sciences, 74, 151-166, 10.1175/Jas-D-16-0087.1, 2017.

Mignani, C., Creamean, J. M., Zimmermann, L., Alewell, C., and Conen, F.: Direct evidence for secondary ice formation at around -15 °C in mixed-phase clouds, Atmos. Chem. Phys. Discuss., under review, 2018.

Morris, C. E., Georgakopoulos, D. G., and Sands, D. C.: Ice nucleation active bacteria and their potential role in precipitation, J Phys Iv, 121, 87-103, DOI 10.1051/jp4:2004121004, 2004.

Morris, C. E., Sands, D. C., Bardin, M., Jaenicke, R., Vogel, B., Leyronas, C., Ariya, P. A., and Psenner, R.: Microbiology and atmospheric processes: research challenges concerning the impact of airborne micro-organisms on the atmosphere and climate, Biogeosciences, 8, 17-25, 10.5194/bg-8-17-2011, 2011.

Morris, C. E., Conen, F., Huffman, J. A., Phillips, V., Poschl, U., and Sands, D. C.: Bioprecipitation: a feedback cycle linking Earth history, ecosystem dynamics and land use through biological ice nucleators in the atmosphere, Global Change Biol, 20, 341-351, 10.1111/gcb.12447, 2014.

Morris, C. E., Soubeyrand, S., Bigg, E. K., Creamean, J. M., and Sands, D. C.: Mapping Rainfall Feedback to Reveal the Potential Sensitivity of Precipitation to Biological Aerosols, Bulletin of the American Meteorological Society, 98, 1109-1118, https://doi.org/10.1175/BAMS-D-15-00293.1, 2017.

Mossop, S. C., and Thorndike, N. S. C.: The Use of Membrane Filters in Measurements of Ice Nucleus Concentration. I. Effect of Sampled Air Volume, Journal of Applied Meteorology, 5, 474-480, 10.1175/1520-0450(1966)005<0474:tuomfi>2.0.co;2, 1966.

Murray, B. J., O'Sullivan, D., Atkinson, J. D., and Webb, M. E.: Ice nucleation by particles immersed in supercooled cloud droplets, Chem Soc Rev, 41, 6519-6554, Doi 10.1039/C2cs35200a, 2012.

O'Sullivan, D., Murray, B. J., Malkin, T. L., Whale, T. F., Umo, N. S., Atkinson, J. D., Price, H. C., Baustian, K. J., Browse, J., and Webb, M. E.: Ice nucleation by fertile soil dusts: relative importance of mineral and biogenic components, Atmos. Chem. Phys., 14, 1853-1867, 10.5194/acp-14-1853-2014, 2014.

O'Sullivan, D., Murray, B. J., Ross, J. F., and Webb, M. E.: The adsorption of fungal ice-nucleating proteins on mineral dusts: a terrestrial reservoir of atmospheric ice-nucleating particles, Atmos Chem Phys, 16, 7879-7887, 10.5194/acp-16-7879-2016, 2016.

Petters, M. D., and Wright, T. P.: Revisiting ice nucleation from precipitation samples, Geophys Res Lett, 42, 8758-8766, 10.1002/2015gl065733, 2015.

Price, H. C., Baustian, K. J., McQuaid, J. B., Blyth, A., Bower, K. N., Choularton, T., Cotton, R. J., Cui, Z., Field, P. R., Gallagher, M., Hawker, R., Merrington, A., Miltenberger, A., Neely, R. R., Parker, S. T., Rosenberg, P. D., Taylor, J. W., Trembath, J., Vergara-Temprado, J., Whale, T. F., Wilson, T. W., Young, G., and Murray, B. J.: Atmospheric Ice-Nucleating Particles in the Dusty Tropical Atlantic, J Geophys Res-Atmos, 123, 2175-2193, 10.1002/2017jd027560, 2018.

Reche, I., D'Orta, G., Mladenov, N., Winget, D. M., and Suttle, C. A.: Deposition rates of viruses and bacteria above the atmospheric boundary layer, Isme J, 12, 1154-1162, 10.1038/s41396-017-0042-4, 2018.

Sahyoun, M., Korsholm, U. S., Sorensen, J. H., Santl-Temkiv, T., Finster, K., Gosewinkel, U., and Nielsen, N. W.: Impact of bacterial ice nucleating particles on weather predicted by a numerical weather prediction model, Atmos Environ, 170, 33-44, 10.1016/j.atmosenv.2017.09.029, 2017.

Schnell, R. C., and Vali, G.: Biogenic Ice Nuclei .1. Terrestrial and Marine Sources, Journal of the Atmospheric Sciences, 33, 1554-1564, Doi 10.1175/1520-0469(1976)033<1554:Binpit>2.0.Co;2, 1976.

Stein, A. F., Draxler, R. R., Rolph, G. D., Stunder, B. J. B., Cohen, M. D., and Ngan, F.: NOAA's HYSPLIT Atmospheric Transport and Dispersion Modeling System, Bulletin of the American Meteorological Society, 96, 2059-2077, 10.1175/bams-d-14-00110.1, 2015.

715 Stopelli, E., Conen, F., Zimmermann, L., Alewell, C., and Morris, C. E.: Freezing nucleation apparatus puts new slant on study of
716   biological ice nucleators in precipitation, Atmos Meas Tech, 7, 129-134, 10.5194/amt-7-129-2014, 2014.
717 Stopelli, E., Conen, F., Morris, C. E., Herrmann, E., Bukowiecki, N., and Alewell, C.: Ice nucleation active particles are efficiently
718   removed by precipitating clouds, Scientific Reports, 5, 16433, 10.1038/srep16433, 2015.
719 Stopelli, E., Conen, F., Morris, C. E., Herrmann, E., Henne, S., Steinbacher, M., and Alewell, C.: Predicting abundance and
720   variability of ice nucleating particles in precipitation at the high-altitude observatory Jungfraujoch, Atmos Chem Phys,
721   16, 8341-8351, 10.5194/acp-16-8341-2016, 2016.
722 Stopelli, E., Conen, F., Guilbaud, C., Zopfi, J., Alewell, C., and Morris, C. E.: Ice nucleators, bacterial cells and Pseudomonas
723   syringae in precipitation at Jungfraujoch, Biogeosciences, 14, 1189-1196, 10.5194/bg-14-1189-2017, 2017.
724 Storelvmo, T., Hoose, C., and Eriksson, P.: Global modeling of mixed-phase clouds: The albedo and lifetime effects of aerosols,
725   Journal of Geophysical Research: Atmospheres, 116, doi:10.1029/2010JD014724, 2011.
726 Suski, K. J., Hill, T. C. J., Levin, E. J. T., Miller, A., DeMott, P. J., and Kreidenweis, S. M.: Agricultural harvesting emissions of
727   ice-nucleating particles, Atmos. Chem. Phys., 18, 13755-13771, 2018.
728 Tesson, S. V. M., Skjøth, C. A., Šantl-Temkiv, T., and Löndahl, J.: Airborne Microalgae: Insights, Opportunities and Challenges,
729   Applied and Environmental Microbiology, 10.1128/aem.03333-15, 2016.
730 Tobo, Y., DeMott, P. J., Hill, T. C. J., Prenni, A. J., Swoboda-Colberg, N. G., Franc, G. D., and Kreidenweis, S. M.: Organic matter
731   matters for ice nuclei of agricultural soil origin, Atmos. Chem. Phys., 14, 8521-8531, 10.5194/acp-14-8521-2014, 2014.
732 Tobo, Y.: An improved approach for measuring immersion freezing in large droplets over a wide temperature range, Scientific
733   Reports, 6, ARTN 3293010.1038/srep32930, 2016.
734 Twohy, C. H., McMeeking, G. R., DeMott, P. J., McCluskey, C. S., Hill, T. C. J., Burrows, S. M., Kulkarni, G. R., Tanarhte, M.,
735   Kafle, D. N., and Toohey, D. W.: Abundance of fluorescent biological aerosol particles at temperatures conducive to the
736   formation of mixed-phase and cirrus clouds, Atmos Chem Phys, 16, 8205-8225, 10.5194/acp-16-8205-2016, 2016.
737 Twomey, S.: The Influence of Pollution on the Shortwave Albedo of Clouds, Journal of the Atmospheric Sciences, 34, 1149-1152,
738   10.1175/1520-0469(1977)034<1149:tiopot>2.0.co;2, 1977.
739 Vali, G., and Stansbury, E. J.: Time-Dependent Characteristics of Heterogeneous Nucleation of Ice, Can J Phys, 44, 477-+, DOI
740   10.1139/p66-044, 1966.
741 Vali, G.: Quantitative Evaluation of Experimental Results an the Heterogeneous Freezing Nucleation of Supercooled Liquids,
742   Journal of the Atmospheric Sciences, 28, 402-409, 10.1175/1520-0469(1971)028<0402:qeoera>2.0.co;2, 1971.
743 Vali, G., Christensen, M., Fresh, R. W., Galyan, E. L., Maki, L. R., and Schnell, R. C.: Biogenic Ice Nuclei .2. Bacterial Sources,
744   Journal of the Atmospheric Sciences, 33, 1565-1570, Doi 10.1175/1520-0469(1976)033<1565:Binpib>2.0.Co;2, 1976.
745 Vali, G., DeMott, P. J., Möhler, O., and Whale, T. F.: Technical Note: A proposal for ice nucleation terminology, Atmos. Chem.
746   Phys., 15, 10263-10270, 10.5194/acp-15-10263-2015, 2015.
747 Vali, G.: Revisiting the differential freezing nucleus spectra derived from drop freezing experiments; methods of calculation,
748   applications and confidence limits, Atmos. Meas. Tech. Discuss., 2018, 1-18, 10.5194/amt-2018-309, 2018.
749 von Blohn, N., Mitra, S. K., Diehl, K., and Borrmann, S.: The ice nucleating ability of pollen: Part III: New laboratory studies in
750   immersion and contact freezing modes including more pollen types, Atmos Res, 78, 182-189,
751   10.1016/j.atmosres.2005.03.008, 2005.
752 Weingartner, E., Nyeki, S., and Baltensperger, U.: Seasonal and diurnal variation of aerosol size distributions (10 < D < 750 nm)
753   at a high-alpine site (Jungfraujoch 3580 m asl), J Geophys Res-Atmos, 104, 26809-26820, Doi 10.1029/1999jd900170,
754   1999.
755 Wex, H., Augustin-Bauditz, S., Boose, Y., Budke, C., Curtius, J., Diehl, K., Dreyer, A., Frank, F., Hartmann, S., Hiranuma, N.,
756   Jantsch, E., Kanji, Z. A., Kiselev, A., Koop, T., Mohler, O., Niedermeier, D., Nillius, B., Rosch, M., Rose, D., Schmidt,
757   C., Steinke, I., and Stratmann, F.: Intercomparing different devices for the investigation of ice nucleating particles using
758   Snomax (R) as test substance, Atmos Chem Phys, 15, 1463-1485, 10.5194/acp-15-1463-2015, 2015.
759 Wilson, T. W., Ladino, L. A., Alpert, P. A., Breckels, M. N., Brooks, I. M., Browse, J., Burrows, S. M., Carslaw, K. S., Huffman,
760   J. A., Judd, C., Kilthau, W. P., Mason, R. H., McFiggans, G., Miller, L. A., Najera, J. J., Polishchuk, E., Rae, S., Schiller,
761   C. L., Si, M., Temprado, J. V., Whale, T. F., Wong, J. P. S., Wurl, O., Yakobi-Hancock, J. D., Abbatt, J. P. D., Aller, J.
762   Y., Bertram, A. K., Knopf, D. A., and Murray, B. J.: A marine biogenic source of atmospheric ice-nucleating particles,
763   Nature, 525, 234-+, 10.1038/nature14986, 2015.
764 Wright, T. P., and Petters, M. D.: The role of time in heterogeneous freezing nucleation, J Geophys Res-Atmos, 118, 3731-3743,
765   10.1002/jgrd.50365, 2013.
766

767 **Table 1. Dates and times for cloud rime, snow, and aerosol samples collected during the 2018 winter INCAS study at Jungfraujoch.** <u>**Also**</u>
768 <u>**shown are the dominant air mass sources (free troposphere or FT or boundary layer intrusion of BLI) for each day based on radon data.**</u>
769 **Samples highlighted in blue and red are the northwest and southeast case studies, respectively.** <u>**Samples highlighted in green represent**</u>
770 <u>**predominantly southerly days that were classified as Saharan dust events (SDEs) or BLI days.**</u>

~~Date~~Date	Air mass	Cloud rime			Snow			Aerosol			Stages
		Sample	Start (UTC)	Duration (hh:mm)	Sample	Start (UTC)	Duration (hh:mm)	Sample	Start (UTC)	Duration (hh:mm)	
15-Feb	FT	Rime1 06:30	03:07		Snow1 07:15	01:15		DRUM1	10:00	12:00	A/B/C/D
		Rime2 09:37	02:13		Snow2 08:40	01:30		DRUM2	22:00	24:00	A/B/C/D
		Rime3 11:50	03:55		Snow3 10:10	01:35					
		Rime4 15:45	03:35		Snow4 12:45	02:30					
		Rime5 19:20	13:55		Snow5 15:20	04:00					
16-Feb	FT	Rime6 07:15	02:10		Snow6 07:15	02:02		DRUM3	22:00	24:00	A/B/C/D
		Rime7 09:29	02:41		Snow7 09:23	02:37					
					Snow8 14:00	17:50					
17-Feb	FT	Rime8 12:08	01:16		Snow9 07:50	02:23		DRUM4	22:00	24:00	A/B/C/D
		Rime9 13:24	02:23		Snow10 10:16	01:10					
		Rime10 15:47	03:12		Snow11 11:35	00:33					
		Rime11 18:59	06:48		Snow12 12:20	01:04					
					Snow13 13:42	01:00					
					Snow14 14:45	00:55					
					Snow15 15:54	02:54					
					Snow16 18:52	05:50					
18-Feb	FT	Rime12 00:47	08:22		*None*			DRUM5	22:00	24:00	A/B/C
19-Feb	FT	Rime13 21:00	10:50		Snow17 21:00	08:50		DRUM6	22:00	24:00	A/B/C
20-Feb	FT	Rime14 05:50	04:14		Snow18 05:50	04:14		DRUM7	22:00	24:00	A/B/C
		Rime15 12:08	02:17		Snow19 12:08	02:14					
21-Feb	FT	*None*			*None*			DRUM8	22:00	24:00	A/B/C/D
22-Feb	BLI	*None*			*None*			DRUM9	22:00	24:00	A/B/C/D
23-Feb	BLI	Rime16 20:00	14:30		Snow20 07:49	02:51		DRUM10	22:00	24:00	A/B/C/D
					Snow21 10:55	03:35					
					Snow22 14:40	02:42					
					Snow23 20:00	12:11					
24-Feb	FT, SDE	*None*			*None*			DRUM11	22:00	24:00	A/B/C
25-Feb	FT	*None*			*None*			DRUM12	22:00	24:00	A/B
26-Feb	FT	*None*			*None*			DRUM13	22:00	24:00	A/B/C
27-Feb	BLI	*None*			*None*			DRUM14	22:00	24:00	A/B/C
28-Feb	BLI	*None*			*None*			DRUM15	22:00	24:00	A/B/C
01-Mar	BLI	*None*			*None*			DRUM16	22:00	24:00	A/B/C
02-Mar	FT	*None*			*None*			DRUM17	22:00	24:00	A/B/C
03-Mar	FT	*None*			*None*			DRUM18	22:00	24:00	A/B/C
04-Mar	FT	*None*			*None*			DRUM19	22:00	24:00	A/B/C
05-Mar	FT	Rime17 16:43	15:32		Snow24 21:52	08:16		DRUM20	22:00	24:00	A/B/C
06-Mar	BLI	Rime18 06:15	03:03		Snow25 06:15	02:50		DRUM21	22:00	24:00	A/B/C
		Rime19 09:18	05:42		Snow26 09:14	05:26					
		Rime20 15:00	02:08		Snow27 14:54	01:56					
		Rime21 17:08	04:41		Snow28 17:26	04:04					
		Rime22 22:38	21:40		Snow29 22:38	07:35					
07-Mar	BLI	Rime23 06:19	03:58		Snow30 06:19	01:19		DRUM22	22:00	24:00	A/B/C
		Rime24 10:17	05:40		Snow31 07:50	02:00					
		Rime25 15:57	08:31		Snow32 12:49	02:59					
		Rime26 22:28	06:34		Snow33 16:00	05:19					
					Snow34 22:28	06:27					
08-Mar	FT	*None*			*None*			DRUM23	22:00	24:00	A/B/C
09-Mar	FT	*None*			*None*			DRUM24	22:00	24:00	A/B/C
10-Mar	FT, SDE	Rime27 11:00	21:46		Snow35 06:00	04:00		DRUM25	22:00	24:00	A/B/C
					Snow36 10:10	01:56					
11-Mar	BLI	Rime28 06:46	02:59		Snow37 05:48	04:03		*None*			
		Rime29 09:56	03:49		Snow38 09:54	03:51					
		Rime30 13:45	04:48		Snow39 13:48	02:28					

771

a) Relative humidity and air temperature
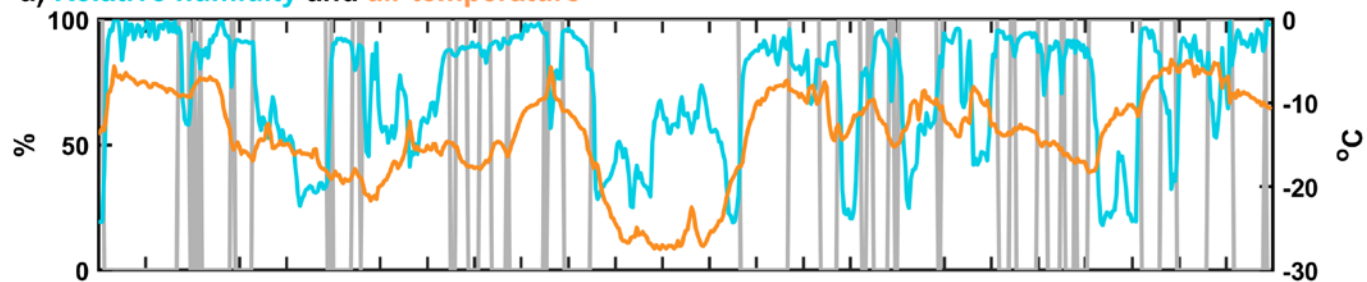
b) Wind speed coloured by wind direction (north, west, south, east)
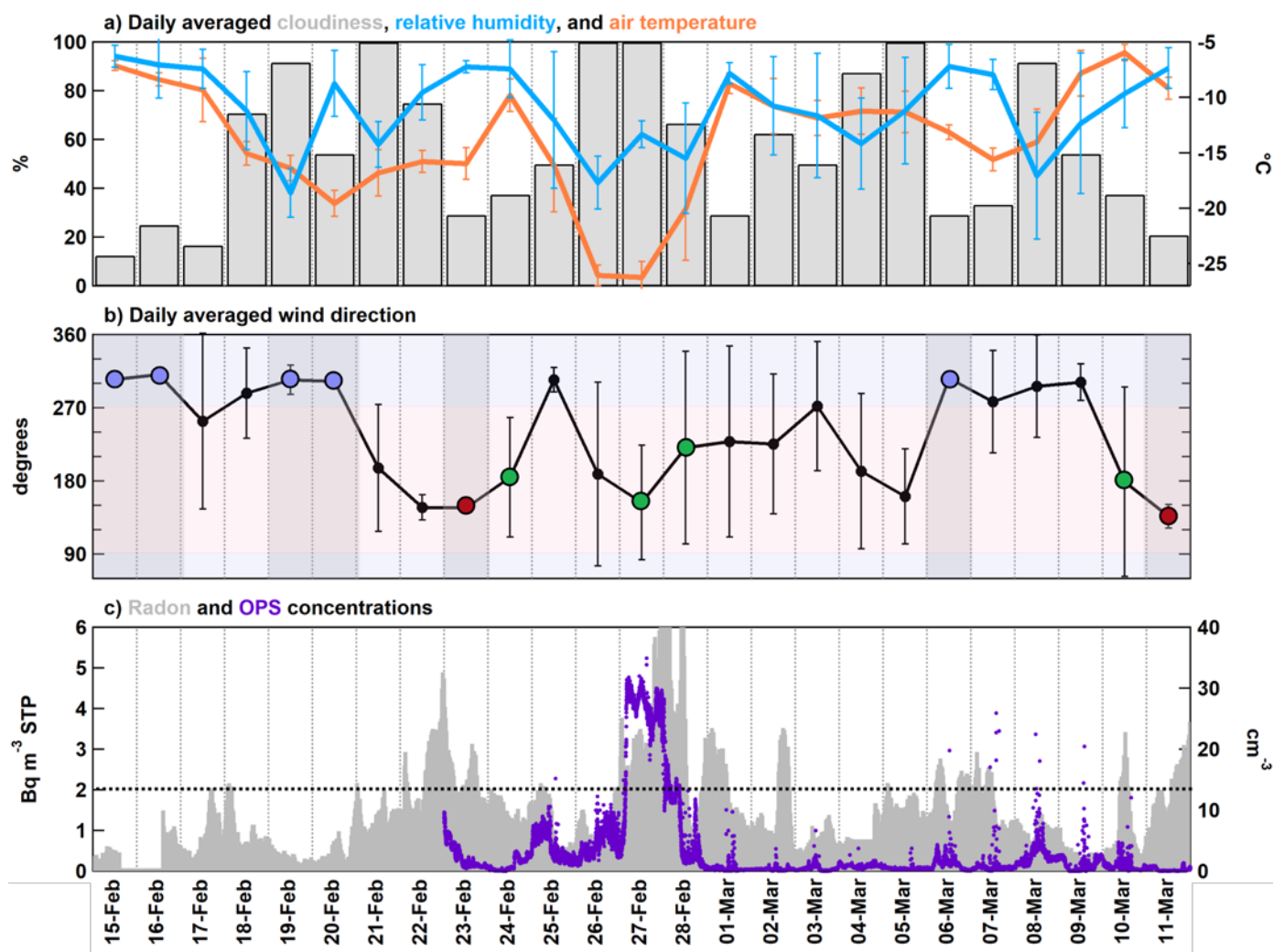
772
773

20
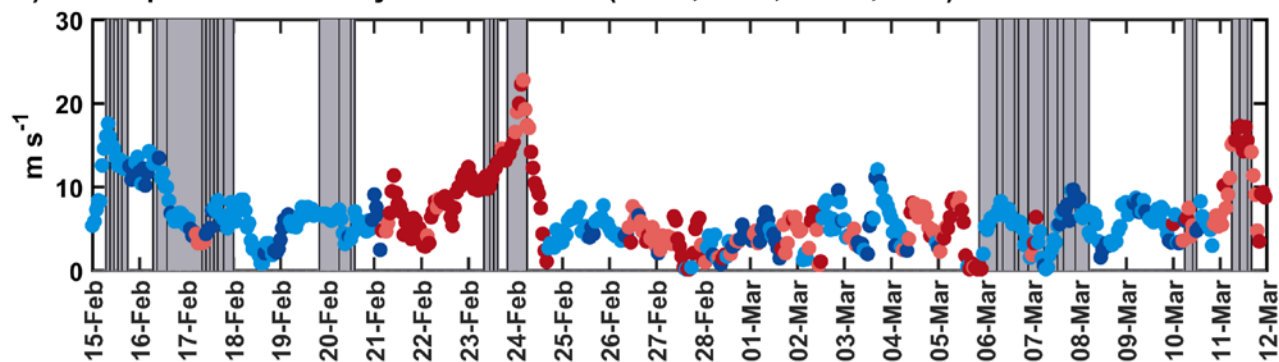
Figure 1. ~~Daily averaged m~~Meteorological data at JFJ from INCAS, including a) percentage of cloudiness in the vertical profile over JFJ per the estimation by Herrmann et al. (2015), station relative humidity (%), and station air temperature (°C) and b) station wind direction. The background of b) is shaded horizontally by north (light blue) or south (light red) directions. Additionally, days with combined aerosol, cloud rime, and snow collections are vertically shaded grey. Blue and red markers for wind direction represent case study storm days that were entirely northwesterly or southeasterly, respectively. Green markers represent predominantly southerly days that were classified as Saharan dust events (SDEs) or heavy boundary layer influence days. c) Time series of radon (^{222}Rn) corrected for standard temperature and pressure and OPS particle concentrations. The black dashed line indicates a threshold of 2 Bq m^{-3} whereby boundary layer intrusion likely occurred at JFJ. OPS data were missing prior to 23 Feb. Error bars represent standard deviation. ~~relative humidity and surface air temperature and b) wind speed colored by wind direction. Grey shading in a) indicates in-cloud measurement conditions per the estimation by Herrmann et al. (2015) and in b) indicates snow and cloud rime collections with the width of the bar indicating the duration of each sample. Aerosol sampling was conducted daily during all conditions (i.e., precipitation, cloudy, and clear sky). North, east, south, and west correspond to wind direction ranges of 315 – 45, 45 – 135, 135 – 225, and 225 – 315 degrees, respectively.~~

21

Probability

m s⁻¹
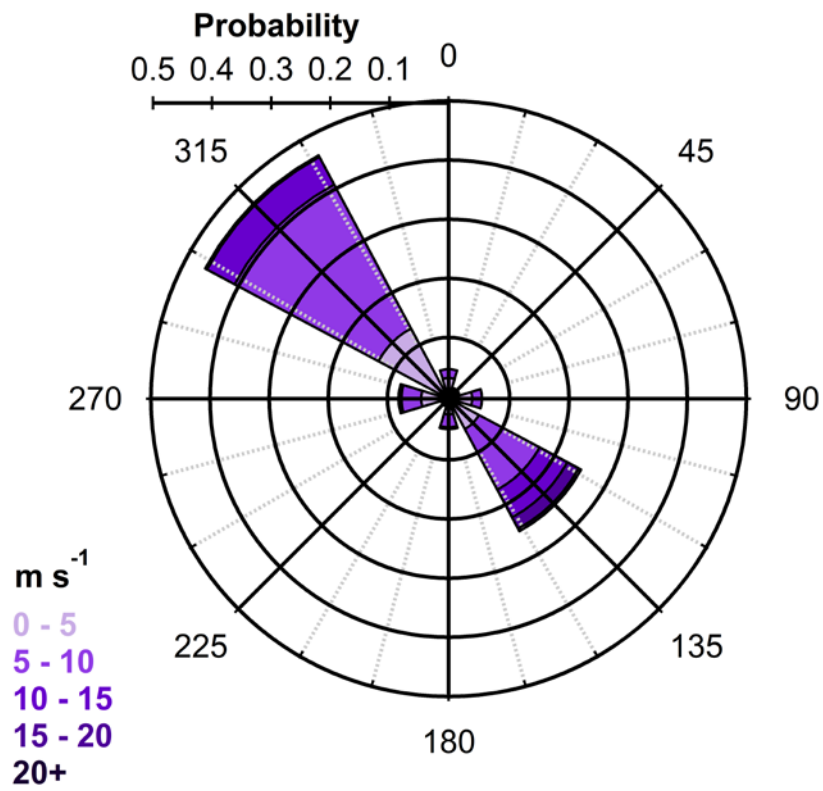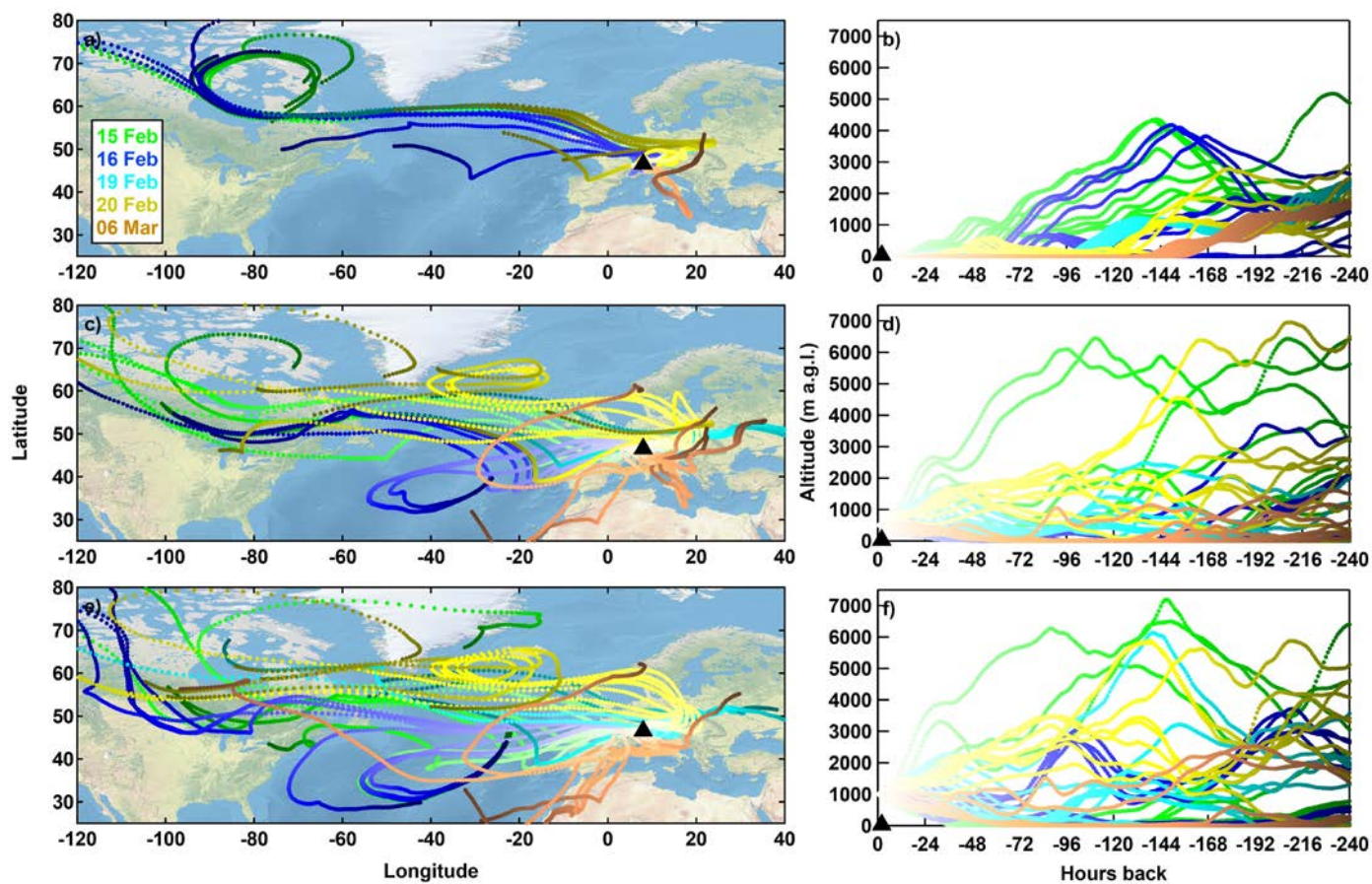
0 - 5
5 - 10
10 - 15
15 - 20
20+

788
789   Figure 2. Rose plot for wind data during INCAS. Values correspond to wind direction binned by 45 degrees and wind speeds binned by
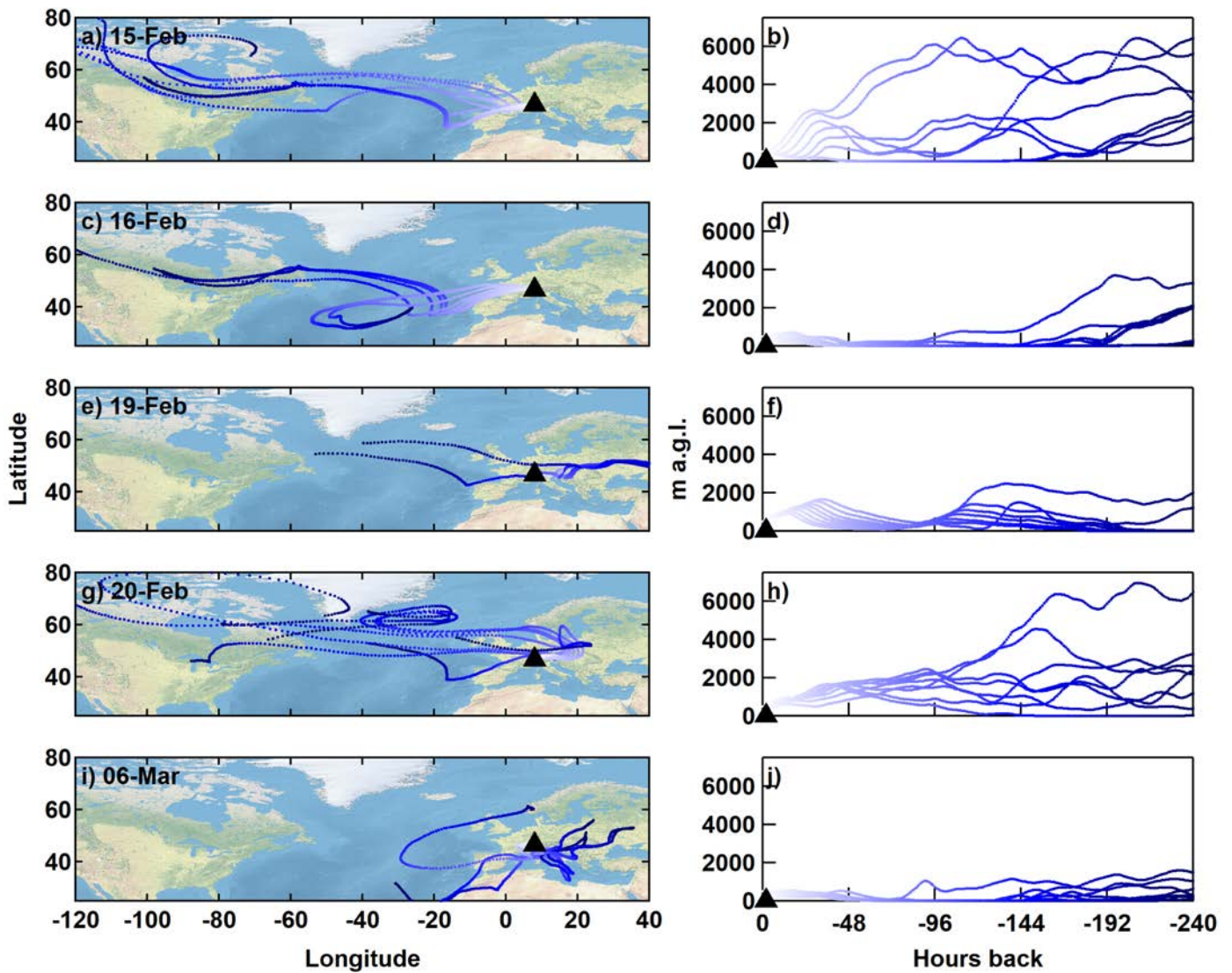790   5 m s⁻¹. The probability for wind speed to fall within these bins is plotted.

22

23

Figure 3. 10-day air mass backward trajectories initiated every 3 hours during sample collection for northwesterly case days ~~ending at~~ 500 m above ground level (a.g.l.). Trajectories are plotted by latitude-longitude (left) and altitude-time (right) profiles for 15 Feb (a, b), 16 Feb (c, d), 19 Feb (e, f), 20 Feb (g, h), and 06 Mar (i, j). Darker shades of blue represent trajectory points farther back in time.~~at a) 10, c) 500, and e) 1000 m a.g.l. Altitude profiles versus time are also shown for b) 10, d) 500, and f) 1000 m a.g.l. Each day is coloured differently to differentiate between the days.~~
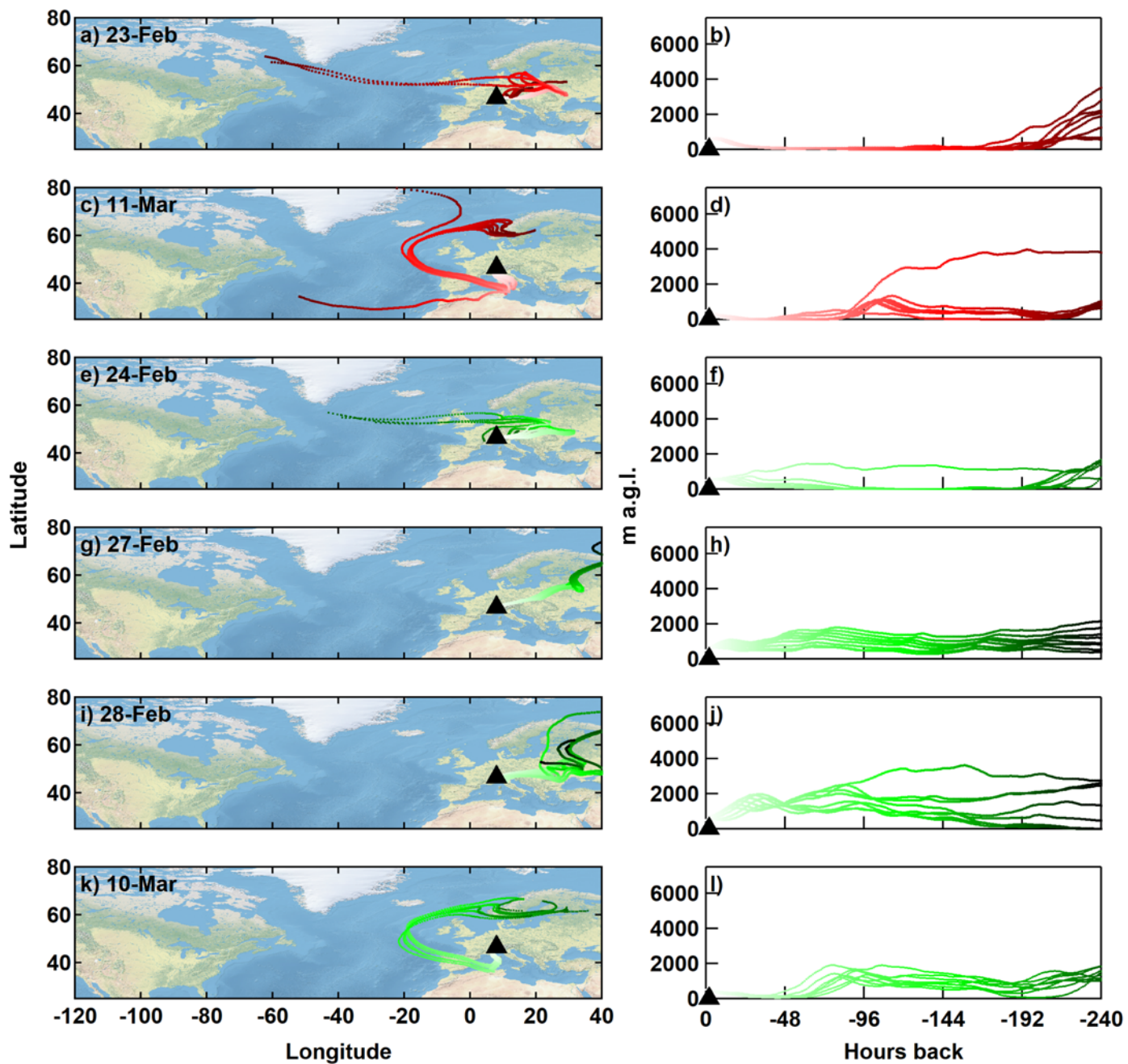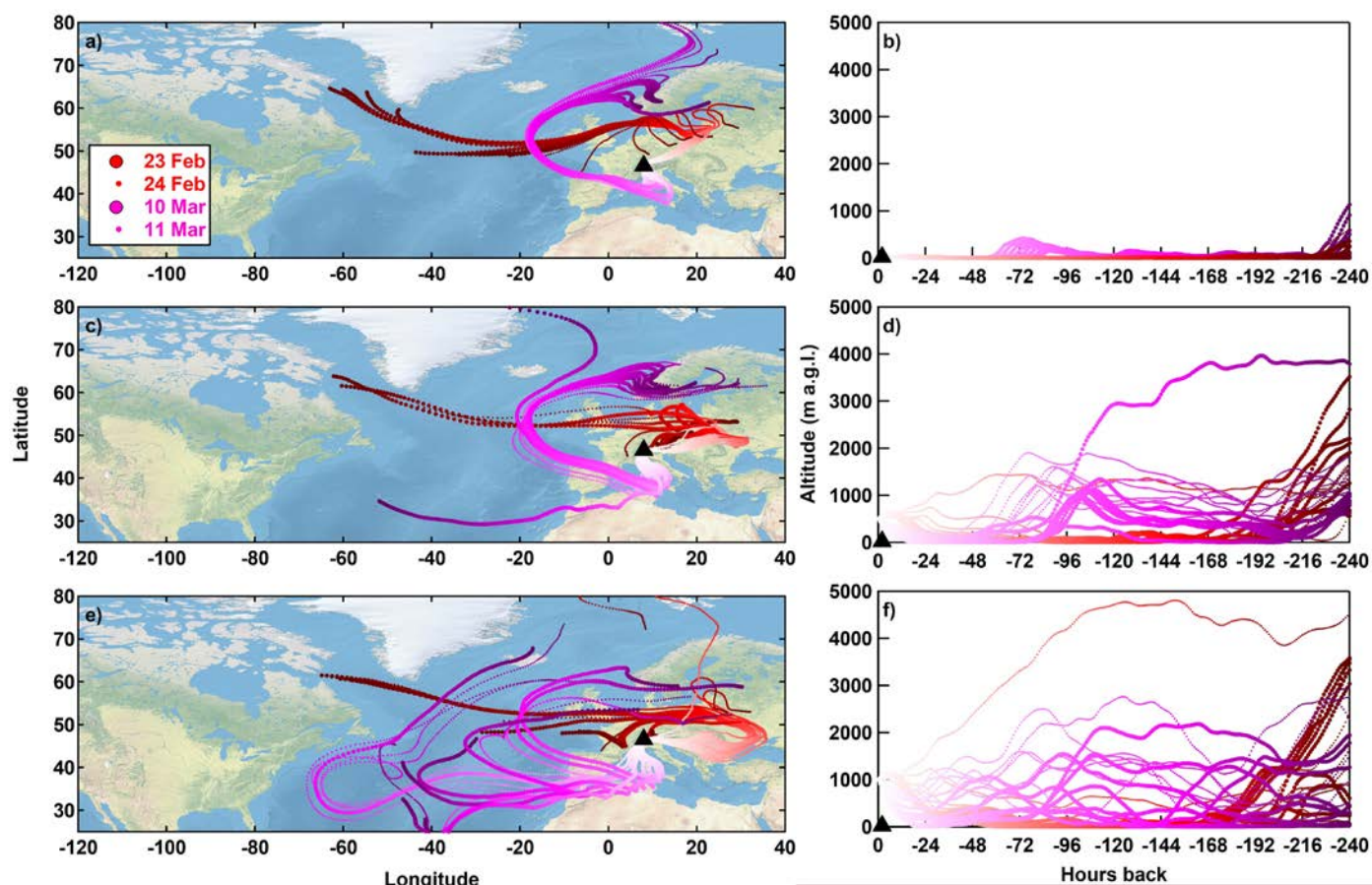
Figure 4. Same as Figure 3, but for southeasterly (23 Feb and 11 Mar), SDE (24 Feb and 10 Mar), and BLI (27 and 28 Feb) case days. 24 Feb and 10 Mar are shown as smaller markers, indicative of possible Saharan dust events from Paul Scherrer Institute.
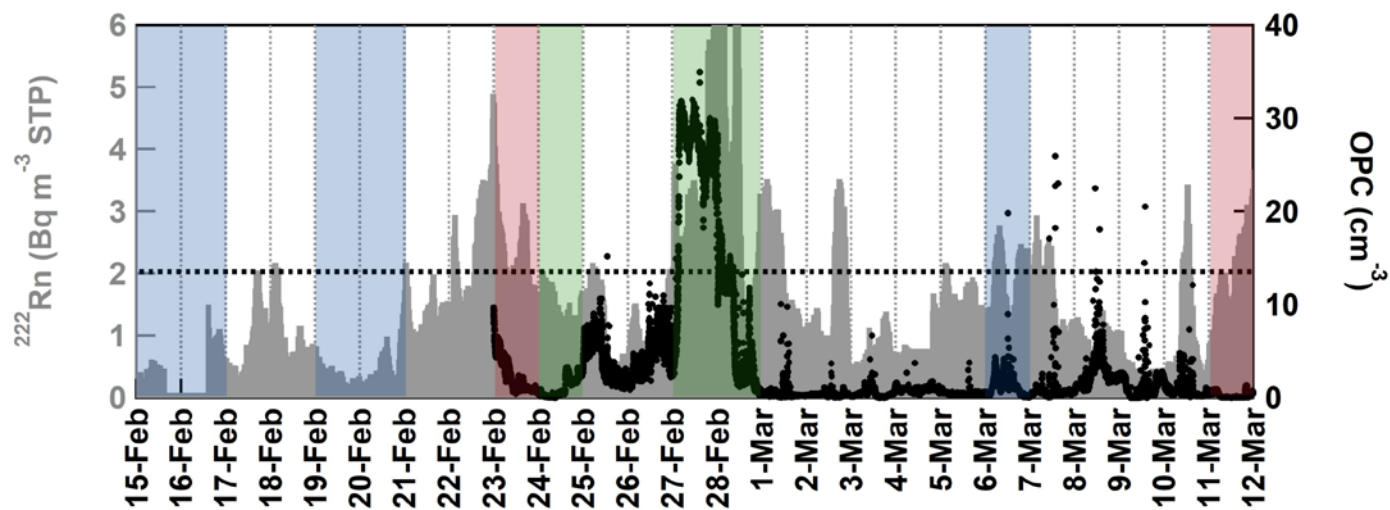
26

Figure 5. ^{222}Rn concentrations (grey) measured and corrected for standard temperature and pressure during INCAS. OPC particle number concentrations (black) are also shown, but data were missing prior to 23 Feb. The black dashed line indicates a threshold of 2 Bq m^{-3} whereby boundary layer intrusion likely occurred at JFJ. Blue and red shadings represent northwesterly and southeasterly case study days, respectively.
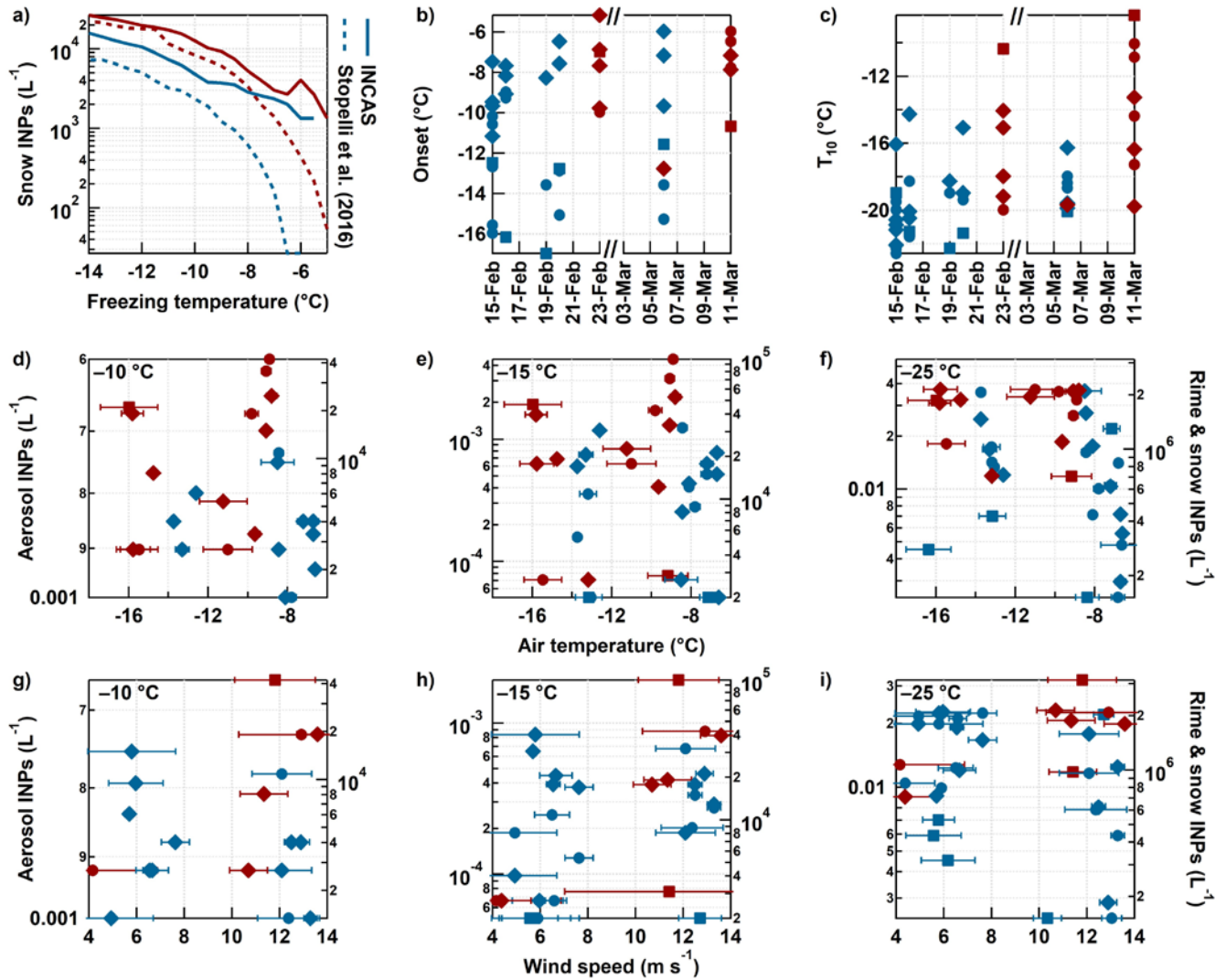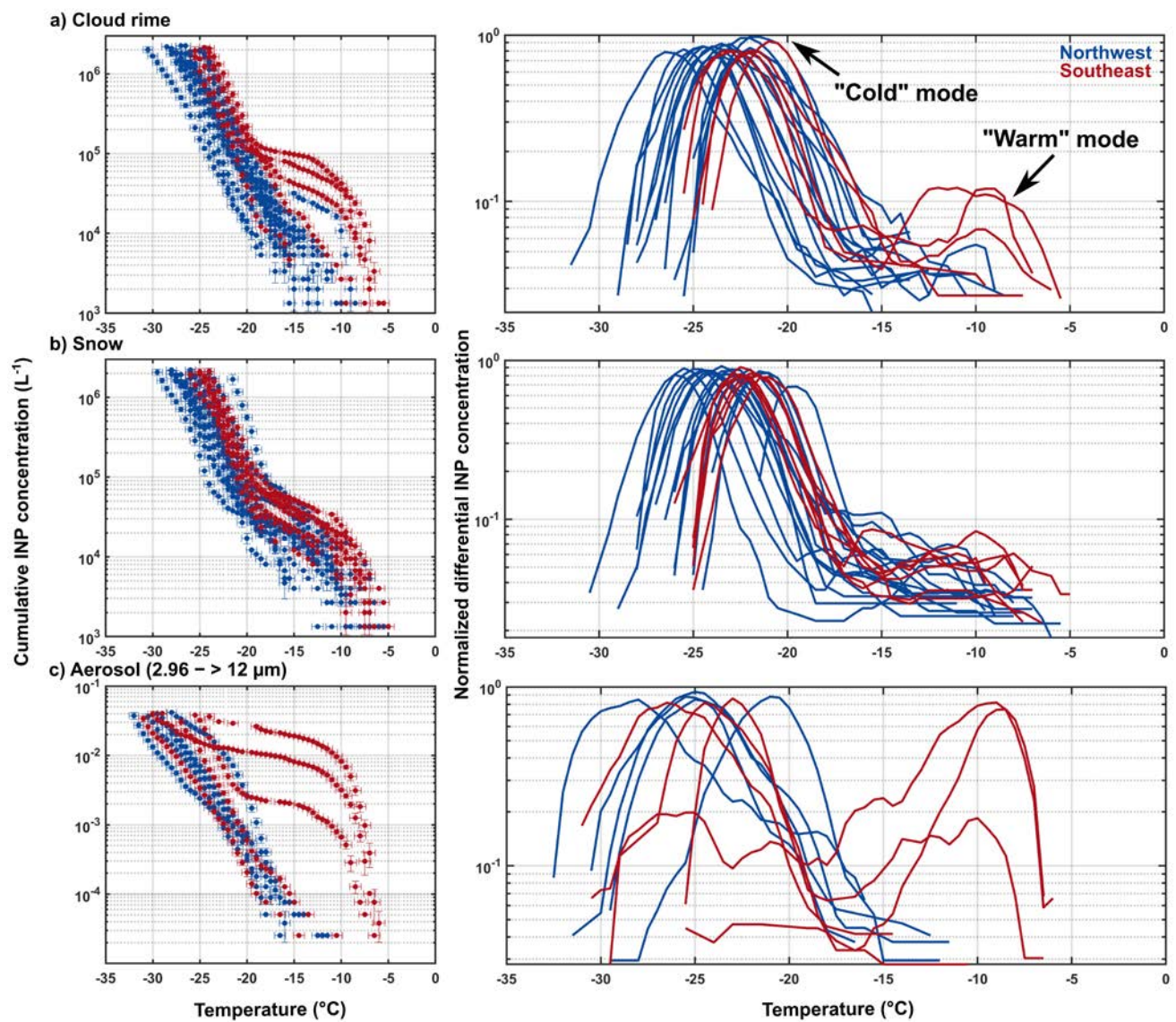
Figure 6. a) Comparison of INCAS snow INPs within the same range of those reported by Stopelli et al. (2016) for measurements at JFJ during the 2012/13 winter season. Summary of INCAS INP concentrations from aerosol (squares), cloud rime (open circles), and snow samples (x's), including b) freezing onset temperatures, and correlations between air temperature averages during sample collection and INPs at freezing temperatures of c) −10 °C, d) −15 °C, and e) −25 °C. The same concentrations at f) −10 °C, g) −15 °C, and h) −25 °C are plotted against average wind speed measured during sample collection periods. Blue and red markers represent northwesterly and southeasterly wind directions, respectively.
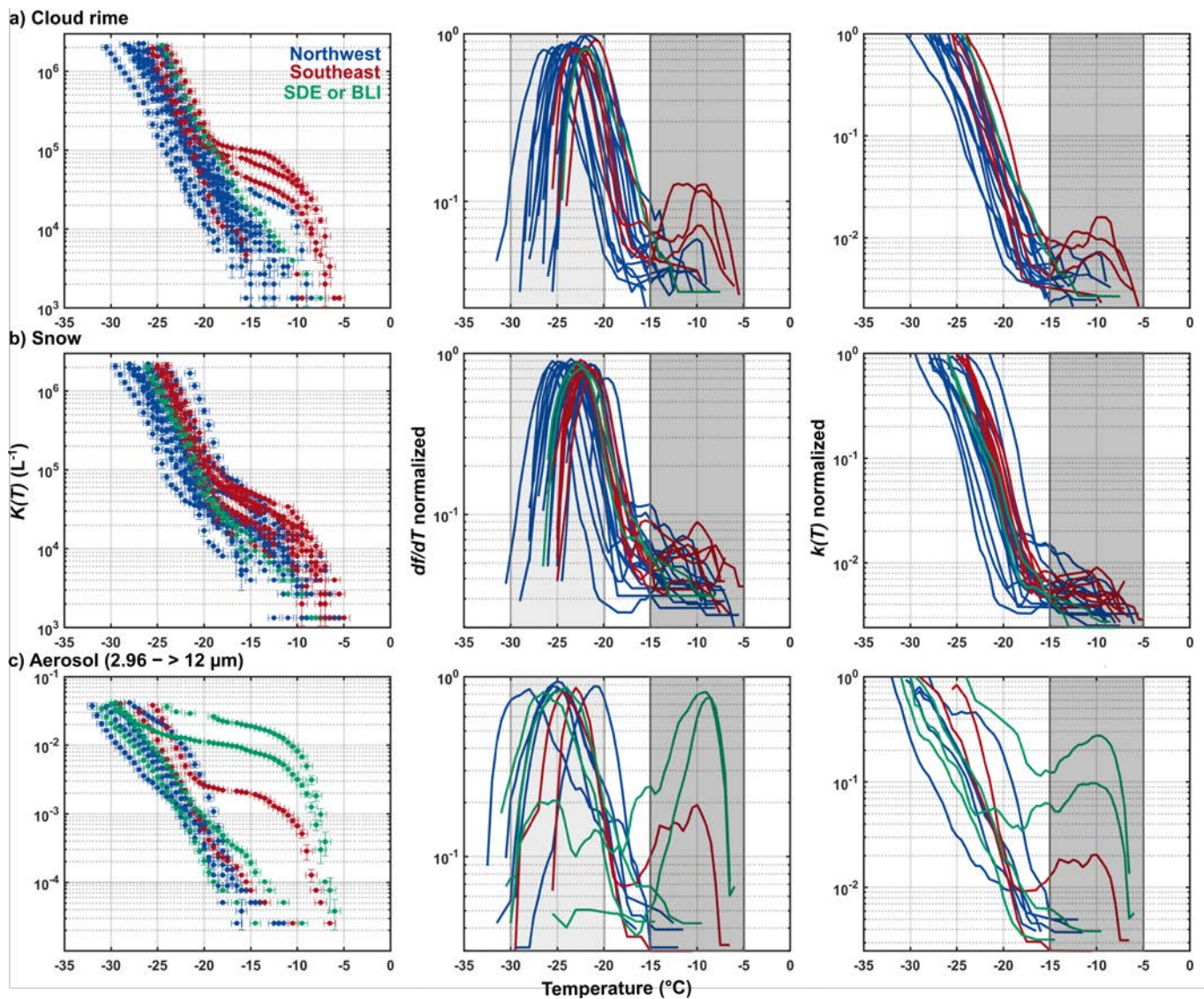
a) Cloud rime

b) Snow

c) Aerosol (2.96 – > 12 μm)

Cumulative INP concentration (L⁻¹)

Normalized differential INP concentration

Temperature (°C)

Temperature (°C)

Northwest
Southeast

"Cold" mode

"Warm" mode

814

29

Figure 75. Cumulative INP spectra (K(T) (, on left), normalized differential of fraction frozen per temperature interval (df/dT), and normalized differential INP spectra (k(T) (, on right) for the same samples of a) cloud rime, b) snow, and c) aerosol for the size range 2.96 − >12 µm in diameter. Spectra shown are for samples from the northwest (blue) and southeast (red) case study dates, in addition to SDE and boundary layer intrusion (BLI) case days (green). Multiple cloud rime and snow samples were collected while one aerosol sample from each size range was collected on northwest and southeast case study days (see Table 1). Additional dates with only aerosol samples (24-Feb and 27-Feb) are also shown in c) (highest of the two modes > =15 °C) and are discussed in section 3.3. TThe "cold" and "warm" mode s areregion is indicated by the dark grey shading in both the normalized df/dT and k(T) INP spectra for cloud rime, for reference, while the cold mode region (for df/dT only) is shown in the normalized df/dT spectra.

824

825

826
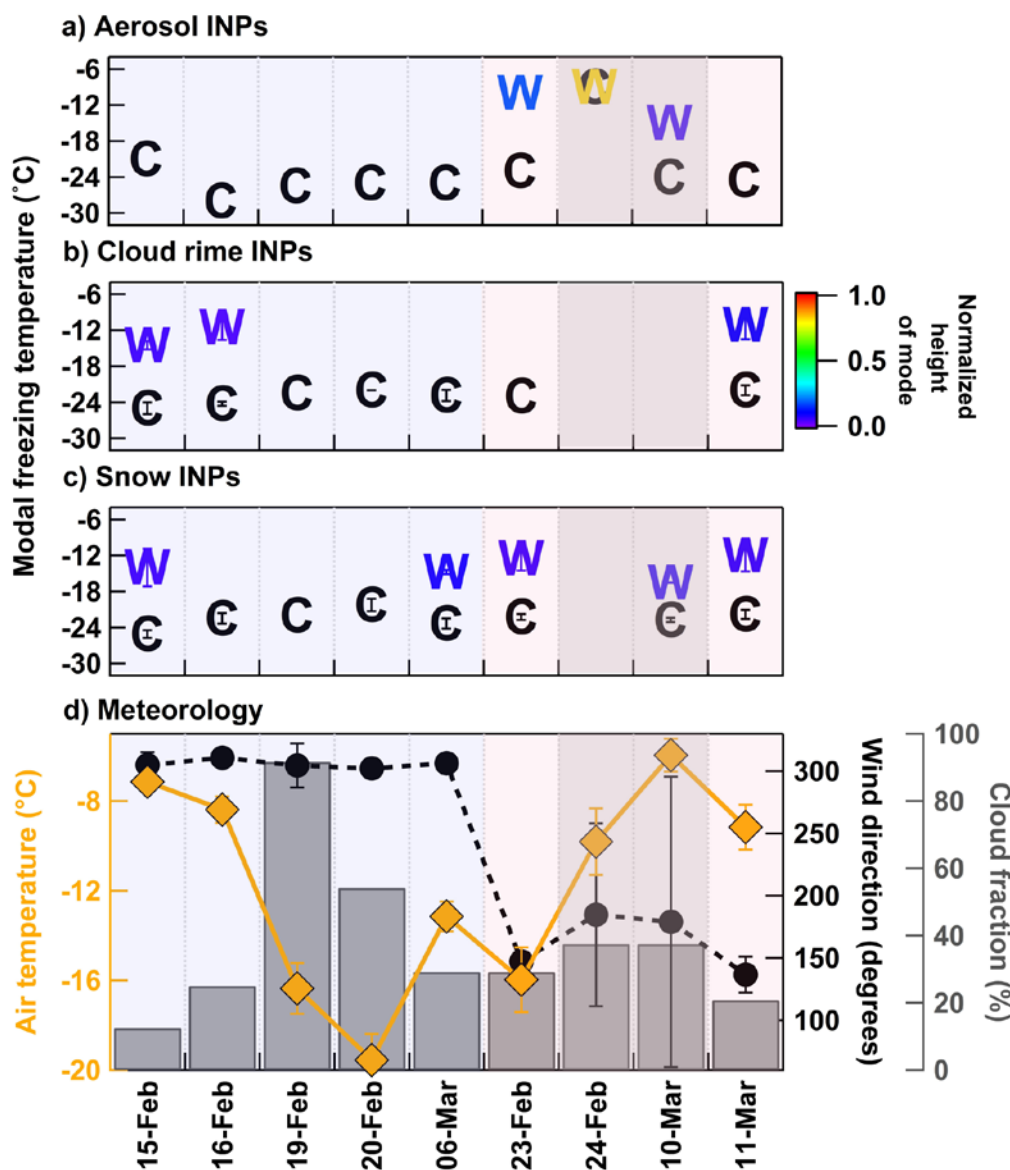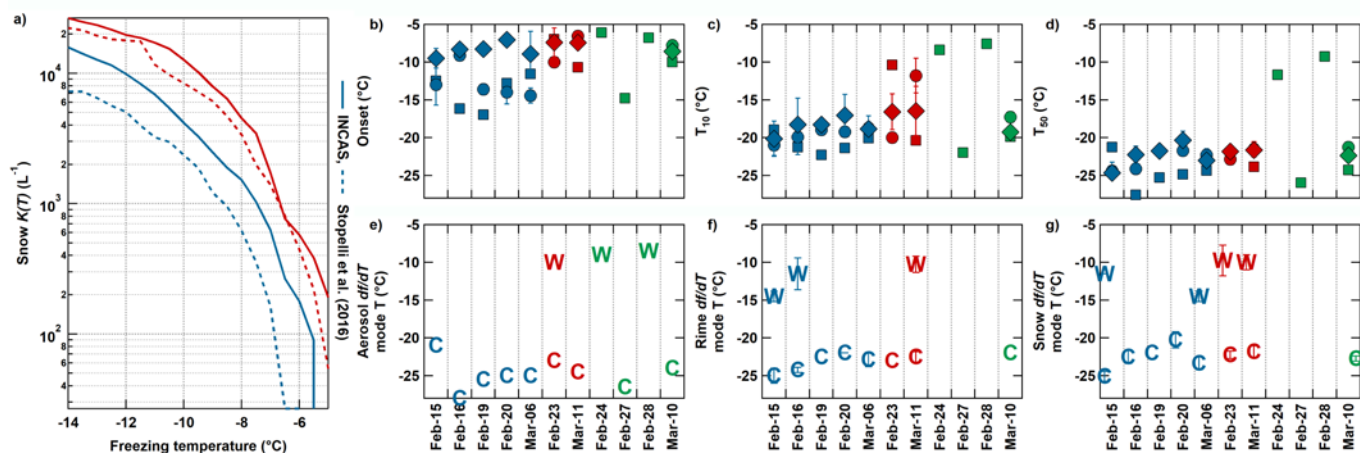
827 **Figure 6. a) Comparison of INCAS cumulative snow INP concentrations for northwest (blue) and southeast (red) within the same range**
828 **of those reported by Stopelli et al. (2016) for measurements at JFJ during the 2012/13 winter season. Summary of INCAS INP**
829 **concentrations from aerosol (squares), cloud rime (circles), and snow samples (diamonds), including b) freezing onset temperatures, c)**
830 **the temperature in which 10% of drops froze, and d) the temperature in which 50% of the drops froze calculated from fraction frozen.**

From the *df/dT* spectra, cold and warm mode temperatures are shown for e) aerosol, f) rime, and g) snow samples. The warm mode temperatures from *df/dT* are the same as for *k(T)*. Blue, red, and green markers represent northwesterly cases, southeasterly cases, and SDE and BLI case days, respectively. Some data points overlap and thus plots may appear to not have the same number of points per sample. ~~Figure 8. Spectral statistics of cold mode height temperature and warm mode height temperatures denoted by "C" and "W", respectively for a) 2.96 –> 12 µm aerosol, b) cloud rime averaged per day, and c) snow averaged per day. Days with only "C" marker indicate the absence of a warm mode. d) shows average air temperature, wind direction, and cloud fraction during the case study days. The days are ordered by northwesterly (blue shading) and southeasterly (pink shading) case days. The southeasterly cases shaded in grey represent days that were not case study days, but days that help explain circumstances of the sampling on 23 Feb and 11 Mar.~~